Dissertations, Master's Theses and Master's Reports - Open | Dissertations, Master's Theses and Master's Reports

2011

Determining bridge deck deterioration through the use of 3D photogrammetry

Darrin C. Evans
Michigan Technological University

DETERMINING BRIDGE DECK DETERIORATION THROUGH THE USE OF 3D
PHOTOGRAMMETRY

By

Darrin C. Evans

A THESIS

Submitted in partial fulfillment of the requirements for the degree of

MASTER OF SCIENCE

CIVIL ENGINEERING

MICHIGAN TECHNOLOGICAL UNIVERSITY

2011

This thesis, "Determining Bridge Deck Deterioration Through the Use of 3D Photogrammetry," is hereby approved in partial fulfillment of the requirements for the Degree of MASTER OF SCIENCE CIVIL ENGINEERING.

Department of Civil and Environmental Engineering

Signatures:

Thesis Advisor _____
Dr. Theresa M. Ahlborn, P.E.

Department Chair _____
Dr. William M. Bulleit, P.E.

Date _____

Table of Contents

List of Figures

List of Tables

Acknowledgments

Abstract

The bridge inspection industry has yet to utilize a rapidly growing technology that shows promise to help improve the inspection process. This thesis investigates the abilities that 3D photogrammetry is capable of providing to the bridge inspector for a number of deterioration mechanisms. The technology can provide information about the surface condition of some bridge components, primarily focusing on the surface defects of a concrete bridge which include cracking, spalling and scaling. Testing was completed using a Canon EOS 7D camera which then processed photos using AgiSoft PhotoScan to align the photos and develop models. Further processing of the models was done using ArcMap in the ArcGIS 10 program to view the digital elevation models of the concrete surface.

Several experiments were completed to determine the ability of the technique for the detection of the different defects. The cracks that were able to be resolved in this study were a 1/8 inch crack at a distance of two feet above the surface. 3D photogrammetry was able to be detect a depression of 1 inch wide with 3/16 inch depth which would be sufficient to measure any scaling or spalling that would be required be the inspector. The percentage scaled or spalled was also able to be calculated from the digital elevation models in ArcMap. Different camera factors including the distance from the defects, number of photos and angle, were also investigated to see how each factor affected the capabilities. 3D photogrammetry showed great promise in the detection of scaling or spalling of the concrete bridge surface.

1   Introduction

1.1   Background

There has been a continued decline in the condition of the bridge infrastructure system as the structures age. According to Federal Highway Administration (FHWA) there are over 600,000 bridges in the United States and of these bridges, almost 70,000 are listed as structurally deficient (Federal Highway Administration (FHWA) 2010). The need for allocating limited resources available for bridge repair and construction is great because more than eleven percent of the nation's bridges are in need of repair. The current bridge inspection process requires all bridge structures to be inspected at least every two years, with bridges showing signs of stress being inspected more frequently. This is done mainly through a visual inspection in which the inspector uses their expertise and past experience to determine the condition of the bridge (American Association of State Highway and Transportation Officials (AASHTO) 2008). With the condition rating highly dependent on the inspector, the subjectivity of this process makes it difficult to gain consistent assessment of the bridge condition.

The use of 3D photogrammetry dates back to as early as the 1840s in which a photogrammetry system was developed by Aime Laussedat (Jiang et al. 2008). Much advancement in this technology has occurred since that period of time. The computer age helped to accelerate the advancement of 3D photogrammetry with the ability to be able to quickly process information. Cameras have advanced significantly to afford higher quality photographs making greater accuracy possible. There have been several computer modeling programs made available to consumers to form 3D models from photographs. But even with the advancements in 3D photogrammetry, little has been done to apply this technology to bridge condition assessment.

1.2   Objective

The objective of this research was to explore the application of the 3D photogrammetry in determining the deterioration of a concrete bridge deck surface. Several different types of deterioration were considered including spalling, scaling and cracking, to determine

1

the degree to which this technology can be applied in evaluating the surface condition. The research considered different factors that could affect the ability to measure these defects including environment, surface conditions, angle of the camera and speed of collection. Capabilities of 3D photogrammetry were investigated to understand what will be able to be measured for the bridge inspection. The best way to supply the deterioration information to the bridge inspector was also considered.

1.3   Content

There are several different aspects that are covered in this evaluation of 3D photogrammetry for condition assessment of bridge decks. The first part is an overview of the literature on what bridge inspectors do during an inspection. Also covered is an overview on the current state of 3D photogrammetry and its limited use in the bridge inspection field. A small scale test was conducted to evaluate this technology's applicability using commercially available equipment and software to determine the impact of influencing factors. The results from this test are covered and show the size of defects can be determined with this equipment. Conclusions of current technology and the future work necessary for broad based implementation are also discussed.

2   Literature Review

There are several different types of bridge deck surfaces used on bridges in the United States and include concrete, steel, bituminous, polymer and timber. The majority of bridge decks in the U.S. are constructed from reinforced concrete. Overlays for decks in a deteriorated state typically consist of concrete or bituminous, which can change the deterioration mechanisms. Given most bridge decks start as reinforced concrete, the inspection procedures for concrete bridge decks will be concentrated on (Chung et al. 1994). Overlays are beyond the scope of this project.

2.1   *Bridge Deck Deterioration Mechanisms*

Several different surface deterioration mechanisms are evaluated to determine the condition of the deck surface and the overall surface roughness which contributes to ride quality.   Deterioration mechanisms include different surface cracks, spalling, scaling, delaminations, voids and expansion joint issues. Each mechanism has its own set of challenges when being measured with 3D photogrammetry. Some mechanisms can be measured directly while others can be measured indirectly through other types of indicators.

Surface cracks come in a variety of different types and widths with different causes behind them. The most common type of crack in bridge decks are transverse cracks which are often caused by restrained shrinkage and typically occur shortly after construction (Nowak et al. 2000). Pattern cracking or map cracking is cracking that occurs in random directions which can be caused by several factors such as freeze and thaw cycles and the steel corrosion process. There are several other varieties of cracks that can be present including longitudinal and diagonal cracks (Nowak et al. 2000). Examples of the main types of cracks can be seen in Figure 2.1(Federal Highway Adminstration (FHWA) 2006). A trained bridge inspector can determine the presence of other problems with knowing the type of cracks present on the bridge.   While the size of the cracks can vary from hairline to several inches, the magnitude of the cracks considered ranged from 1/16 in. (1.59 mm) to 3/16 in. (4.76 mm) in width (FHWA 2006).

| Transverse Crack | Longitudinal Crack | Map (Pattern) Cracking |
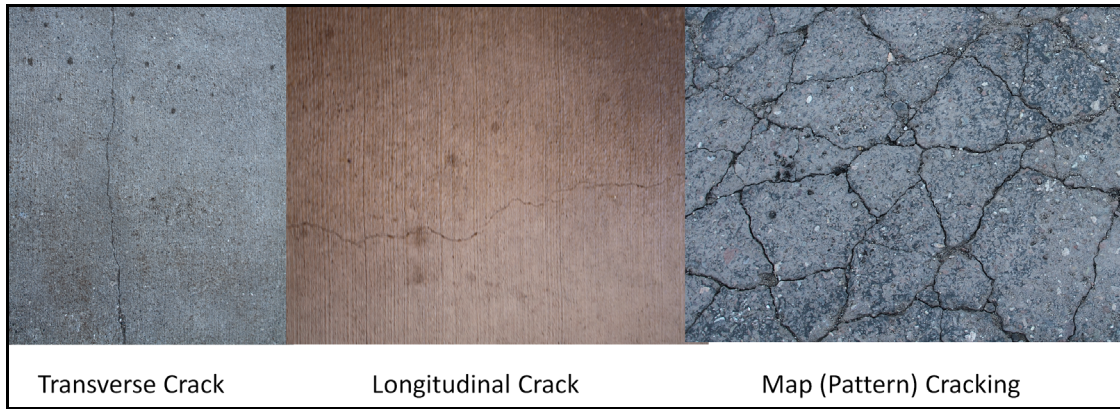
Figure 2.1: Different Crack Types

With cracks not only is the width and length of the cracks considered, but also the amount of cracks in a certain section of roadway. Crack density is defined as the linear feet of cracks in a given section of highway. Michigan Department of Transportation has defined the crack densities for bituminous pavement as listed in Table 2.1. The measurements allow for the grasp of what level densities are looked at when assessing pavement condition, which is similar to bridge decks (Reay et al. 1998). Crack density measurement can be as important as the width of the crack in assessing the condition of the structure. High crack density can be linked to material failure that typically requires replacement (FHWA 2006).

Table 2.1:
Crack Density Definitions

Density	Linear Crack Length per 100 m Pavement Section	Linear Crack Length per 100 ft Pavement Section
Low	< 10 m	< 10 ft
Moderate	10 m to 135 m	10 ft to 135 ft
High	> 135 m	> 135 ft

The next deterioration mechanism appears when corrosion occurs on the reinforcing steel causing expansion of the reinforcing steel. This triggers the concrete to crack around the corroded rebar leading to delaminations above the rebar. Once the concrete above the delamination breaks away from the surface, it leaves a hole in the surface creating a spall.

An example of spalling on a concrete bridge deck can be seen in Figure 2.2. Scaling is a deterioration mechanism similar to that of spalling with different sources for the material loss. Scaling is an issue with the deck surface that is caused by a loss of material due to material degradation as seen in Figure 2.3. The magnitude of ¼ in. (6.35 mm) in depth is the minimum considered with spalling and scaling measurements when a bridge inspector is recording the deck condition (FHWA 2006).

Figure 2.2: An Example of a Spall

Figure 2.3: An Example of Scaling

There are several different issues related to the expansion joints of the bridge. These include torn or missing seals, armored plate damage, chemical leaching on the bottom of a joint, cracks within two feet of the joint, and spalls within two feet of the joint (FHWA 2006). With the cracking and spalling, it is at the discretion of the inspector if these were caused by an expansion joint failure.

Another issue with concrete bridge decks is the overall surface roughness. Resulting from a combination of several deterioration mechanisms, overall roughness of the bridge deck is important for the traveling public's perception of bridge quality. Roughness in pavement is typically reported using an International Roughness Index (IRI) which was developed to help standardize the roughness measurement (Gillespie 1992). This system measures the variation from the longitudinal profile of the roadway surface to that of a smooth surface in inches per mile of the roadway to relate how much variation is in a section of road. Typical values range from 0 inches per mile to 300 inches per mile on an extremely rough road. The ASTM E1926 – 08 is used as the standard for determining IRI measurements. This measurement is typically not considered during a bridge inspection as this information is not available to the inspector for each particular bridge deck.

2.2   Standard Bridge Inspection Procedure

Bridge inspection is an important process of assessing the current condition of a structure and is used by the state and local transportation agencies as a basis for determining safety and remaining service life along with maintenance, repair and rehabilitation schedules. There are several different methods and types of inspection techniques that are implemented for the inspector to gain an understanding of the condition of the structure. The most common inspection techniques are visual and advanced. Types of inspections include initial, routine, hands-on, fracture-critical, underwater, in-depth, scoping, damage, or special inspections (NCHRP 2007).

Even though a variety of methods are used by the bridge inspector in performing the inspections of the bridges, all inspections must be fulfilled in accordance with the

National Bridge Inspection Standards (NBIS). To help the bridge inspector with programs, procedures and techniques for inspecting bridges, Federal Highway Administration (FHWA) and the National Highway Institute (NHI) produce the Bridge Inspector's Reference Manual (BIRM) (FHWA 2006). All bridge inspectors are required to complete a NHI comprehensive training program at the beginning of their career to become certified. This certification has to be kept current through refresher courses throughout their career.

All publicly-owned bridges must be inspected a minimum of every two years to be in compliance with NBIS. If a particular bridge is determined to be susceptible to increased deterioration, more frequent inspections may be required. The National Bridge Inventory (NBI) requires that any bridge with a span greater than twenty feet must be rated and recorded in the inventory. If the condition of the bridge requires load rating, the inspection reports provide the details for capacity calculations which can lead to weight limits being posted on the structure. For a transportation agency, bridge condition affects maintenance and repair schedules, but it also influences allowable load limits and ride quality for vehicle traffic, all of which significantly impact the public's experience and perception of the current state of the U.S. bridge infrastructure.

In the current bridge inspection process, the primary method used by bridge inspectors is visual evaluation. Visual evaluation of the structure is done during a routine inspection of the bridge and advanced techniques are not used unless the inspector recognizes some abnormality which requires more evaluation. The bridge inspection process is highly subjective and relies on experience-based expertise that must be developed over the years through practice. This process has been refined over forty years, but still lacks consistency in establishing condition of bridges. Establishing the condition of the bridge deck is still subjective as the quantity of scales and spalling size is sometimes measured with a ruler and the percent area is estimated by the inspector. Cracks are typically noted by the bridge inspector, and no action is usually taken besides checking the concrete around the crack with an inspection hammer to ensure it is solid. Also, delaminations cannot be seen, but are located by hammer sounding or chain drag.

2.3   Advanced Bridge Inspection Techniques

Several different techniques have been developed to help the bridge inspector gain a more accurate assessment of bridge deck condition. Because the majority of the bridge decks in the U.S. are constructed from reinforced concrete (Chung et al. 1994), this will focus on the inspection procedures for concrete bridge decks. Several techniques have been available to the bridge inspector for a long time with the main two being chain drag and core sampling. In recent years there has been a surge in developing nondestructive test methods with some of the main methods including ground-penetrating radar, impact-echo and infrared thermography (FHWA 2006). These tests focus on trying to determine exactly what is happening under the surface, but also have potential in resolving surface deterioration mechanisms.

Chain dragging is a tried and true non-destructive inspection technique for bridge inspectors to locate the presence of delaminations in the concrete bridge deck. The chain dragging technique works by dragging chains across the bridge deck surface while the inspector listens to the acoustic response. The locations of delaminations are located by the distinctive hollow sound produced by chains when in contact with delaminated concrete. Having the inspector listen to the response from the chains can lead to this technique being subjective such that different inspectors can obtain conflicting results. However, this is still a fairly accurate technique even given the subjectivity of it (Gastineau et al. 2009). One of the main disadvantages of this technique is a lane closure is required.

Core sampling has the ability to allow the inspector to see the extent of deterioration under the surface by removing material from the deck. Coring is often used by the bridge inspector to verify the results from a nondestructive test performed on the bridge deck (FHWA 2006). This can be a time consuming process with having to bring in equipment to take the cores. The coring process also requires having to close lanes of traffic to do the sampling and is destructive. Depending on the location and number of cores, the strength of the bridge deck can be compromised, making it a process that inspectors tend to try and limit to cause the least amount of impact as possible to the bridge deck.

Ground-penetrating radar (GPR) has been documented by many studies for its use in the evaluation of bridge decks (Gastineau et al. 2009). This radar operates within the radar bands that allow the radar waves to penetrate the material. The radar waves are transmitted into the bridge deck with the reflections of the waves being picked up by antennas. These responses are then processed by a computer and are shown as images which require a skilled user to identify any deterioration mechanisms in the deck. A main concern with this technology is in implementing it in a more user-friendly way for the typical bridge inspector. GPR has been shown to detect a variety of different defects including cracks, voids and delaminations in concrete, and corrosion of the reinforcing steel (Gastineau et al. 2009). There are many companies that perform GPR inspections of the bridge deck, but this technology has not progressed to where the average bridge inspector can use it for typical inspection. There are several disadvantages with GPR such as the difficulty and subjectiveness in the interpretation of the data. Also, data collection with either a manual system or one mounted on a vehicle require a lane closure, although there has been improvement on increasing the speed in which data can be collected (Scheff 2000). This technology has shown to be effective in several areas, but has yet to be consistently implemented on typical bridge inspections.

Impact-echo is a technique which involves the striking of the surface while listening to the response. Impact-echo equipment typically consists of wheels which incorporate both a striker and a microphone to detect the response. Based on the response from the bridge deck the instrument can differentiate if the concrete is intact or there is some defect present. The depth of the defect can be found if the response indicates a depth in the slab less than the depth of the actual slab (Gastineau et al. 2009). There are a variety of subsurface defects that can be detected using this technique including delaminations, voids, grout voids, cracks or other subsurface anomalies in the bridge deck. There are two positives with this technique in that it is highly accurate and that the defect depths can be calculated to get a better condition assessment. Disadvantages with the technique are that many points need to be tested and traffic needs to be stopped while the collection of data is taking place. The interpretation of data can require specialized programs and

training to be able to accurately assess the deterioration of the bridge deck (Gastineau et al. 2009).

Infrared thermography is used to detect the anomalies in the concrete bridge deck based on the thermal conductivity of the concrete. The camera is designed to pick up the thermal infrared spectrum showing the difference in radiant temperature of the concrete surface. The thermal conductivity of the concrete makes the detection of defects possible as the defect acts as an insulator limiting the conduction of the thermal energy. Thermal temperature difference between an area of sound concrete and that of damaged concrete is then able to be seen.

There are several advantages in using infrared thermography as it is portable and has been shown to operate at highway speeds. Processing of the images is relatively simple and straight forward allowing recognition of the problematic areas with little to no processing of the data. Shortcomings for infrared thermography are that it depends on the environmental conditions and has a limited depth at which defects can be seen. Infrared thermography requires a change of air temperature to work leading to a couple time periods each day which are favorable for the collection of data. The surface texture can also affect the readings of the technology; oil spots or other debris can affect the results and possibly give false information. This technology has shown promise in the ability to detect defects such as delaminations in the concrete deck, but could possibly best be utilized in connection with other technologies to obtain the best results.

Crack monitoring using 2D images has been completed for pavement monitoring of cracks where classifying the number and type of cracks present is possible. Typically this is done through a technique called gray scale detection. Grey scale detection works based on the fact that concrete cracks are typically darker than the surrounding area, allowing for the cracks to be classified by type, width and length (Sohn et al. 2005). Subjective in nature as the software recognizes the cracks and automatically classifies the crack type making for inaccurate assessments at times. This type of monitoring approach has typically been limited to pavement classification and not to bridge decks. The ability

to implement this technology has been demonstrated by a number of different projects such as those completed by Xu et al. (2003), Ito et al. (20xx) and Furuta et al. (2006).

2.4   Basics behind Photogrammetry

3D photogrammetry has been around for over 150 years starting with the stereo overlapping of photos viewed to provide a 3D image. The beginning of photogrammetry came from the work done by Aime Laussedat in using terrestrial photos to develop maps (Jiang et al. 2008). This technology was first recognized as a viable approach by the Science Academy in Madrid in 1862. One of the biggest moments for photogrammetry's development occurred in 1910 when the International Society for Photogrammetry was formed (Jiang et al. 2008). As the advancement of this technique has continued, it has typically been looked at as a terrestrial technique such as modeling historical buildings, rather than an actually close range technique for capturing detailed features of an object.

Algorithms have been developed to form 3D images from 2D images. The most common method is the least squares method, which has several versions that have developed to determine the location of the same point in the two photographs. Different variations of the least squares method are in practice with each having its disadvantages and advantages, with the linearized least squares method being common (Yilmaz et al. 2008). Other methods have been explored, but the least squared method remains the most popular. Techniques that align photos automatically use point and edge recognition, through which the vectors to the point or edge are compared to those from each of the photographs to obtain a position for the particular point or edge (Gruen et al. 2005).

The advents of computers and digital photography have greatly increased the ability to process large amounts of data for quick and accurate creation of 3D point clouds from the data. The modern age of 3D photogrammetry started through the use of aerial photography in developing topographical maps from photos. 3D photogrammetry has been applied to closer ranges which include applications in accident recreation, architecture, biomechanics, chemistry, biology, archaeology, automotive and aerospace (Jiang et al. 2008). Several programs have been developed to create close range models

for the user. These programs include, but are not limited to, PhotoModeler, AgiSoft PhotoScan, Imagemaster, DigiCad 3D and iWitnessPro.

As the ability to process photos has increased at an exceptional pace, so have the capabilities of the cameras taking the photos which are being processed. The first cameras used in photogrammetry were metric cameras specifically designed for photogrammetry purposes. After that, methods were developed which use standard film cameras in the creation of 3D models. As digital cameras came into the photogrammetry scene, an increase in the image resolution became available to be processed by the programs. This significant increase in resolution directly contributed to a great increase in the accuracy that the models could achieve. Medium to high end cameras record the settings such as focal length, ISO (light sensitivity) and pixels the image was captured with to help the model create a more accurate model.

Off the shelf programs available to the engineer have greatly improved over the years with the ability to form 3D models using photogrammetry. The first programs required extensive input by the user to form accurate models, often requiring the user to identify many points and/or surfaces in the photos to allow the program to produce a model. With some of the newer programs, this has been eliminated by improving the programs ability to determine similar points with recognition software. This provides a much quicker processing of the models, allowing for more applications of this technology.

The expected accuracy with 3D photogrammetry varies based on a variety of different factors. A retro-reflective target provides greater accuracy compared with that of surfaces which diffuse light. Placing the camera closer to the surface will also increase the accuracy. Resolution of the camera also affects the accuracy; however, this is limited by the resources available to the user as higher resolution cameras are more expensive. The algorithms and techniques used by the particular program also can have an effect on the accuracy which can be achieved by the technique.

2.5 *Photogrammetry Application in the Bridge Inspection Field*

Maas and Hampel (2006) completed a study of looking at the use of photogrammetric techniques in the civil engineering field. The focus of their study was on measuring the deflections of materials including bridge decks and girders. This study concluded the expected precision to be obtained in the controlled conditions of the lab to be about 1:100,000 while the theoretical precision that can be obtained to be on the order of 1:250,000. Sub pixel image analysis operations can reach accuracies of 0.01 pixel to 0.05 pixel, but lens distortion on wide angle lenses will often be around five to ten pixels making achieving this accuracy not possible with wide angle lens. With edge detection techniques, they were able to detect cracks that had a width on the order of 0.00012 in. (3 μm) as the cracks in the specimen were forming during testing.

Armesto et al. (2008) presented work on the capabilities of using close range photogrammetry in the detection and monitoring of structural damage. Two different aspects considered were obtaining the dimension of the defect such as cracks that have damaged the structure, and how to interpret the results obtained. This study considered the bootstrap method when analyzing the statistical significance of the results. A survey of cracks was obtained in their study by using a calibrated Canon EOS 10D digital camera with 6.3 megapixel resolution. The cracks were modeled using Delaunay Triangulation. Using the bootstrap method, a confidence interval for this model of 95 percent was found. This showed that the values of crack dimensions where approximately plus or minus 62 in^2 (0.04 m^2) for this study.

Benning et al. (2004) presented work where the crack monitoring on a structure was accomplished using photogrammetry. Using the photogrammetric software, PHIDIAS, cracks were monitored by measuring the displacement of targets placed on the structure. The cracks were with a precision of up to 0.00012 inch (3 μm). Three cameras were used to measure the displacements of the targets. Once the displacements were measured, the crack widths were extracted using a computer to analyze the movements between the targets. Using this method, cracks on the order of 0.0002" to 0.00039" (5 to 10 μm) were resolved.

3   Methodology

3.1   Equipment Used for Testing

One of the main pieces of equipment used in 3D photogrammetry for the collection of data to be analyzed by a photogrammetry program is the camera. There are a variety of considerations that need to be taken into account when looking at what camera is required to achieve the desired results. The main considerations in selecting a camera are cost, resolution, shutter speed and type. Another component of the camera system is the lens on the camera which can vary depending on the application for which it is being deployed.

A large array of cameras are available to be used in photogrammetry with the cost of these varying from twenty dollars to thousands of dollars. The cost of the camera will be a consequence of the parameters that are required for the particular application. Camera cost has decreased significantly compared to the resolutions that are able to be achieved, making 3D photogrammetry more viable. This decreasing cost trend will continue as with most technological products making this an increasingly attractive option in the future.

One of the main considerations when determining what is required for the application is the resolution of the camera. Camera resolution is the number of pixels in the image and is typically listed in megapixels. A great increase in the resolution of cameras over the years has occurred as the number of megapixels that can be place on a sensor of the same size has significantly increased. The more condensed the pixels on a sensor, the more noise that is introduced into the photo. Showing that when selecting a camera, the most important aspect is not just the number of pixels, but also the density of the pixels on the sensor need to be considered when determining what accuracy can be achieved with 3D photogrammetry.

For 3D photogrammetry application in bridge condition assessment, the shutter speed needs to be considered, especially if the information needs to be captured at a fast rate of speed. In this study the speed at which the collection can be taken could be a factor in

determining the feasibility of 3D photogrammetry. Speed at which the camera can collect high resolution photos is important in determining speeds that could be reached while driving across a bridge and still get sufficient coverage of the surface. The rate at which the camera would have to take photos while driving at 60 mph (95 km/h) would be about 11 pictures per second to get sixty percent overlap at 11 ft (3.35 m) above the road surface.

The cost and capabilities of the camera will be a consequence of the parameters that are required for the particular application. At the lower end are the "point and shoot" type cameras available in with many different options and sizes. This is the most common type of camera with many people already owning one that could be used with applications not desiring the highest accuracy. Point and shoot cameras, that are produced now, use a LCD preview screen which shows the image that is to be taken eliminating one of the issues that was present with the film cameras as the actual image the camera was taking a picture of was not shown. The reason high accuracy is more difficult to achieve has to do with the size of the sensor compared to the number of pixels in the image. These cameras can achieve a high number of megapixels, but the density is high creating more noise when modeling with the accuracy suffering as a result. Another component that can lead to diminished accuracy with these cameras is the lack of a fixed focal length. An automatic zoom makes it difficult for the modeling programs to calculate measurements from the photos. The advantages to this type of camera are the relatively low cost along with the physical size which makes for easy portability.

The next type of camera would be a single-lens reflex (SLR) camera which allows the operator to also see the image that is being taken through a system of mirrors. This system is popular with many professional photographers for several reasons including less shutter lag along with the ability to interchange parts e.g. (different lens) making the camera more versatile. One of the advantages of the SLR camera is having a bigger sensor size than "point and shoot" cameras allow for taking photos with higher megapixels and less density, results in greater accuracy while reducing the noise in the image. Another advantage is the ability to change lens giving more versatility to the

15

camera for getting the best picture quality for a particular scenario. SLR cameras are able to take more pictures per second with the faster shutter speed. The disadvantages to the SLR camera are its larger size and increased cost.

The other camera considered was a high speed camera which uses a charge-coupled device (CCD) or a complementary metal–oxide–semiconductor (CMOS) image sensor to take pictures at high rates of speed. A rate of speed of approximately 100,000 frames per second has been recorded for one of these cameras (Pankow et al. 2010). This speed is achieved by decreasing the pixel size of the images, but shows the capability that these cameras have achieved and the possible future improvements in technology. The advantage with these types of cameras is the rate of speed collection that can be completed. Increased speed could allow the technique to be used at full highway speeds. Disadvantages are the cost and size of these cameras. The size makes them difficult move by the operator such that they are often mounted in one position.

The camera that was chosen for this project was the Canon EOS 7D. A high-performance digital SLR camera with a CMOS sensor has about 18 effective megapixels along with capabilities to take approximately 8 frames per second during continuous shooting. Determined to have the best overall properties for the applications in this study, yet affordable enough while providing the necessary speed and resolution. For determining the capability photogrammetry can provide in determining deterioration mechanisms in bridges. Figure 3.1 shows the camera that was used for taking all the images that were used in the modeling applications in this study.

Figure 3.1: Canon EOS 7D Camera

The final important component of a camera is the lens. More the case for the SLR cameras because the lens can be changed whereas the point and shoot type cameras typically have fixed lens. Lens come in a wide variety varying from fish eye lens, which are 8-10 mm of focal length, to ultra zoom which can reach 400 mm of focal length. With the 3D modeling program, a fixed focal length provides better accuracy than one which varies because the program takes focal length into account when computing measurements. The zoom on the lens typically should be kept the same for all the pictures used in a particular model to make sure the highest accuracy can be achieved. For the measuring of deterioration mechanisms on bridge decks in this study, an ultra wide lens with a fixed focal length of 20 mm was chosen to provide the best coverage area while maintaining the desired accuracy.

3.2   3D Modeling Software

Several modeling programs were considered for determining the most suitable one for bridge condition assessment. Different aspects to the programs need to be considered for each 3D modeling programs. These include accuracy that can be achieved from the

17

program, user interface in the program, alignment of the photos, what the modeling program was designed for modeling and whether the program converts the information into the desired format. Determining the influence of these factors can be difficult without thorough examination.

Accuracy that can be achieved from a program is almost impossible to determine given all the different factors that can affect the accuracy for a particular model. The algorithms that a program uses to develop the model can affect the accuracy, but due to the proprietary nature of the programs algorithms are not revealed to the user. Therefore, the only way to assess the difference in accuracy of the programs is to run the same model on the programs being compared. This is cost prohibitive when trying to determine which program would be better for bridge condition assessment because the purchase of the programs being compared would be required; therefore, comparisons were made for several programs based on manufacturer information. Program interface had to be compared in the same way as accuracy.

A couple of ways are available for programs to align the photos in forming a 3D point cloud from the images. One way is to actually pick points that are recognizable in both of the overlapping photos that allow the software to start with accurate points for the model. The number of points required to be picked varies by program, but the greater the number of points in each pair of photos, the more likely the program is to accurately create a point cloud of the surface. Another method is an automatic image recognition system in which the software automatically aligns the photos. Automation allows for quicker processing of images with little operator input into the program. This can also result in inaccurate processing of the images which can be a disadvantage with this method, but the speed of processing is clearly an advantage.

Certain programs have been design with a particular application in mind, but can be utilized for other applications. Of the programs that were considered, some were designed for general 3D modeling while others are designed for specific applications such as accident recreation or architecture. A user will find that a program designed for a

particular application will typically give better results than one that was designed for another application. Data processing may be accomplished in that particular program or data may need to be exported to a different program to process the model. Particular programs will output the data in different file formats, so given what programs want to be used after modeling may make one program better than another.

AgiSoft PhotoScan was the program chosen to complete the work for this study (AgiSoft LLC. 2010). The user interface of the program is shown in Figure 3.2. One of the factors that led to the decision to use AgiSoft PhotoScan was that it uses automatic image recognition to align the photos being processed. Processing the images in the program takes varying amounts of time depending on variables such as the number of images used and the computing power of the computer. One option within the program to speed up the process is to mask the parts of the photo that do not need to be modeled thereby decreasing the complexity of the model. Masking also allows the program to concentrate on modeling the desired area. Once the points for the model have been calculated, a model can be generated from the point cloud using several different options.
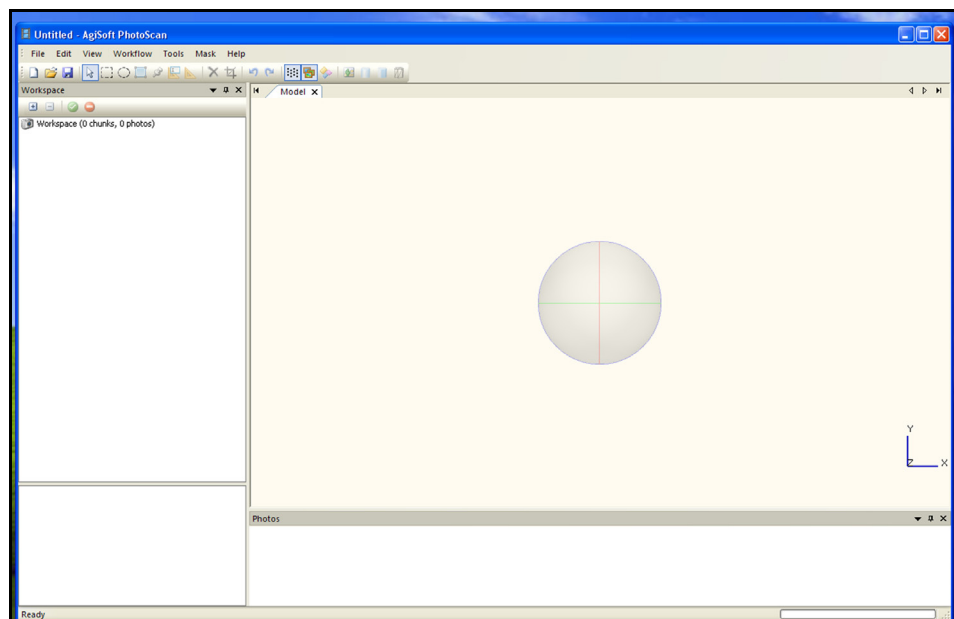
Figure 3.2: Screen Shot of AgiSoft Program

Options for constructing a model are chosen based on what type of resolution or accuracy is required for the modeling application. Modeling options include exact, smooth, height field and fast. The prompt menu with the available options is shown in Figure 3.3. The exact method is more accurate and does not introduce extra geometry such as hole filling. Smooth method is used to generate a surface with little or no holes which creates extra geometry and can be removed later on by the user. Height field method is ideal for modeling of planar surfaces and uses the automatic hole filling option. The final one is the fast method which is faster than the rest and is similar to the smooth method as extra geometry is created.
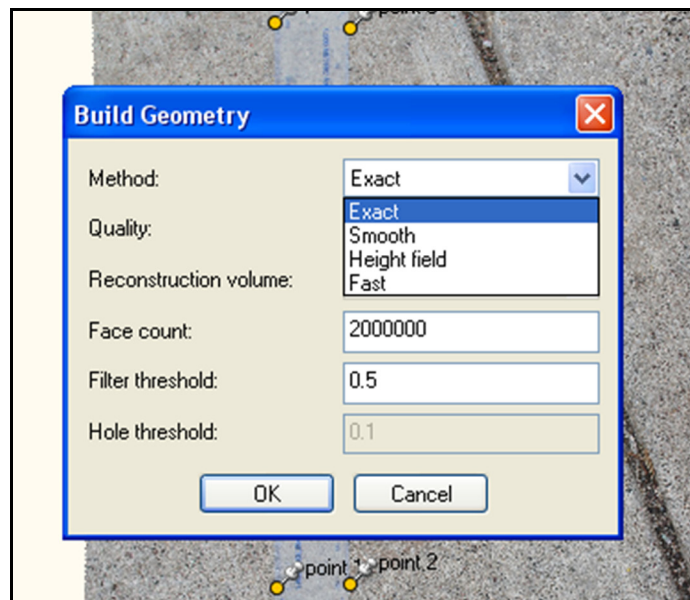
Figure 3.3: Building Geometry Method Options

Several different quality parameters can be chosen in the reconstruction volume options being ultra high, high, medium, low and lowest. These parameters affect the overall quality of the model along with the computing time to process the model. Along with quality, the number of faces in the model has to be chosen by the user which can be any number the user desires, but the greater the number of faces the longer the processing. Filter threshold also has to be chosen by the user which affects the number of faces that can be placed on a small connected component to be removed after the surface

reconstruction. The program contains a hole threshold that can be used with some methods to allow the user to specify the largest sized hole to be filled in.

The different options were reviewed and the best options were chosen to create a 3D model based upon the desired model accuracy of the output for the model and the amount of computing power being used. This is a balancing act that needs to be decided upon by the user to achieve the best and most efficient results for the modeling for the particular application. Keeping this in mind, the chosen parameters for the modeling done in this study included choosing the exact method for reconstructing the surface model and medium quality was chosen to help increase the speed the processing that could be completed. The program default values were used for face count and filter threshold which were 200000 and 0.5, respectively. The final selections can be viewed in Figure 3.4.
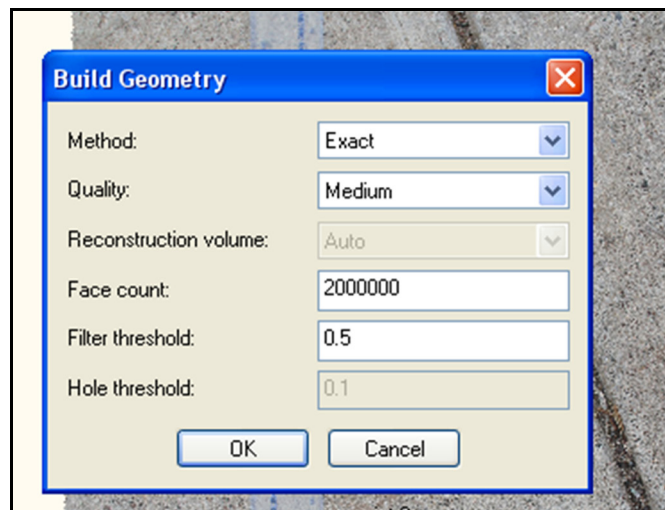
Figure 3.4: Building Geometry Final Selections

Once the model is complete, texture can be added to the model to create a surface that looks like the actual one. Texture mapping is completed automatically by the program in which several options are available. Options include several texture mapping modes which are generic, orthophoto, adaptive orthophoto, single photo and keep uv. Generic mapping mode is the default option in the program which tries to create as uniform texture as possible. In orthophoto mode, the principal plane of the object geometry is
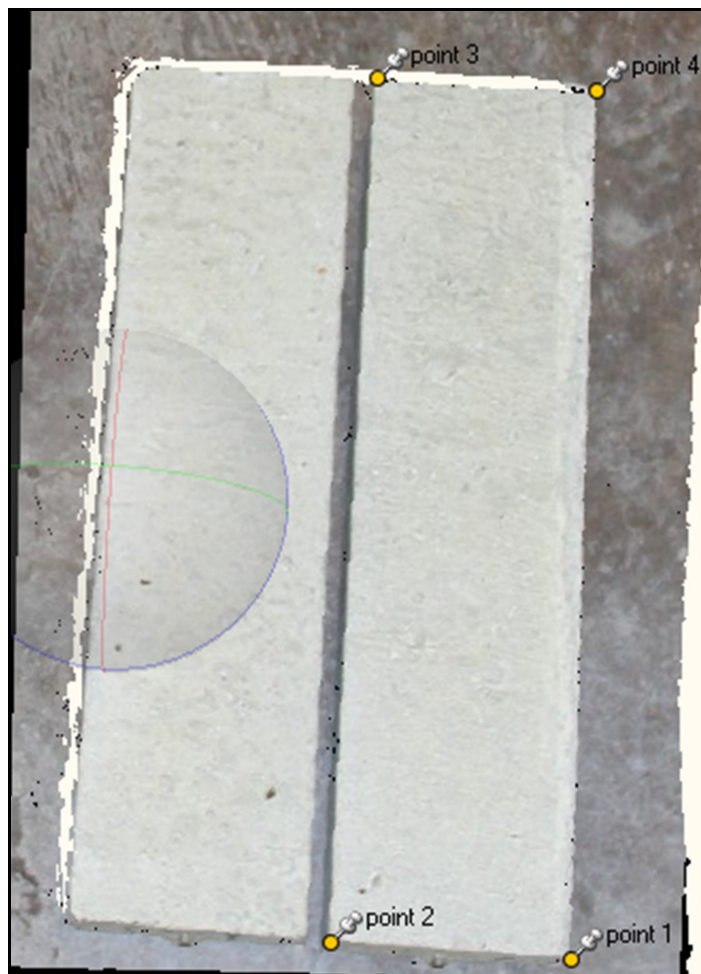
used to generate the texture. This tends to create a more compact texture representation for nearly planar models. The single photo option uses a single photo for creating the texture which can allow for a more realistic look, but it also can create distortion in the texture.

The AgiSoft PhotoScan program also has generation parameters that are chosen by the user including the type of blend mode for the generic mapping and orthophoto mode which include average, "max intensity" and "min intensity". Corresponding pixel value for the texture is chosen by taking the average value of the pixels and the minimum and maximum each taking the corresponding pixels. Atlas width and height can also be chosen to specify the number of pixels in the texture in each of the corresponding directions. This allows the user to choose the desired resolution. Establishing an accurate location of the model points is important for the next step. Creating a digital elevation model (DEM) from the model in which coordinates need to be set up by picking known points in the model. The parameters chosen with this study were generic with max intensity along with keeping the default atlas width and height (2048 pixels each) which can be viewed in Figure 3.5.
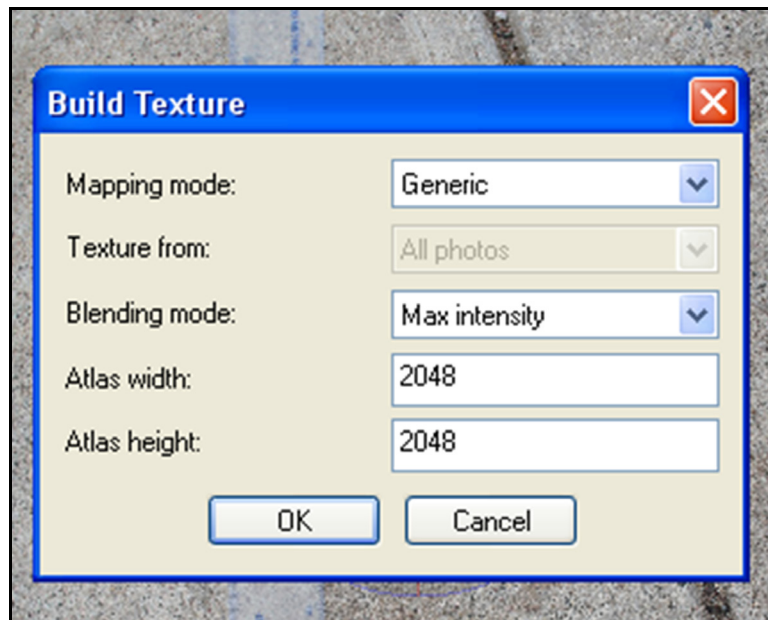
Figure 3.5: Building Texture Final Parameters

The DEM is setup through the user making points on the model that are recognizable and have known measurements. Figure 3.6 shows an example of four points that were marked in the model. Once marked, a keypoint file is created in which the coordinates of the points are given, allowing the program to accurately align all the points. An example of a keypoint file is shown in Figure 3.7 with the coordinates for four points set up. Creating accurate coordinates of the points inside the model where before the values could be measured, but are only correlated to each other not to actual measurements. This allows the model to be opened in a variety of 3D modeling programs for further analysis (See Section 3.5).

Figure 3.6: Points Marked in AgiSoft to Create DEM

Figure 3.7: Example of a Keypoint File

3.3   Testing Process for Crack Width Experiments

Experiments were preformed used a specimen consisting of two concrete blocks that were placed side by side. The concrete blocks were 4 in. (10.2 cm) by 15.5 in. (39.4 cm) with a depth of 3 in. (7.6 cm). These blocks were then moved apart at 1/8 in. (3.18 mm) increments to simulate cracks in the concrete. A camera was placed 24 in. (61 cm) from the specimen and moved laterally across the specimen taking photos at different locations to provide overlap in the photos. The first experiment was completed using these specimens taking five photos of each spacing. Fifteen photos of each spacing setup were used to complete the second experiment. All photos were taken with the Canon camera using a tripod to ensure quality photos that could be replicated.

These images were imported into the AgiSoft PhotoScan software program where the modeling process was completed in accordance to the earlier section. To speed up the process, the images were masked to just contain the specimens and not the floor of the lab. Markers were placed on the four corners of one of the concrete blocks for which a keypoint file was made with the coordinates for each of the corners. Once the points are

defined by the keypoint file, the model was then brought into another program to analyze the results of the experiment. The outputs from these experiments show the capabilities of the technology and help establish a baseline for future experiments. These outputs include such aspects as what size cracks can be measured by the technology and the number of photos that give the best results.

The next experiment was completed in a similar manner to the first one, except that the camera was moved farther back from the concrete blocks to see the capabilities at a greater distance. Designed to show what measurements could be resolved if one or two cameras were used to take pictures of the full width of a highway lane. The camera field of view coverage based on the standoff distance from the specimens is shown in Table 3.1. Formulas used to calculate the values in Table 3.1 were obtained from equation 3-1. The angular field-of-view values for this camera and lens were obtained from Edin (2006) which were 58.28 degrees in the horizontal direction and 40.86 degrees in the vertical direction. This experiment was completed twice; one at each of the two heights determined based upon a typical lane width of 12 ft (3.66 m). The first one was 11 ft (3.35 m) as the distance required for the camera and lens to cover the width of the lane by itself. 5.5 ft (1.68 m) was used for the second experiment as at this height two cameras could cover the width of the lane.

$$FOV = 2*SOD*\tan\left(\frac{AFOV}{2}\right)$$
3-1

where:

       FOV = Field-of-View
       SOD = Standoff Distance
       AFOV = Angular Field-of-View

Table 3.1:
Camera Coverage Based on Distance

Camera Coverage Based on Distance					
Stand Off		Field-of-View			
Distance ft		Horizontal		Vertical	
ft	m	ft	m	Ft	m
1	0.30	1.12	0.34	0.75	0.23
2	0.61	2.23	0.68	1.49	0.45
3	0.91	3.35	1.02	2.24	0.68
4	1.22	4.46	1.36	2.98	0.91
5	1.52	5.58	1.70	3.73	1.14
6	1.83	6.69	2.04	4.47	1.36
7	2.13	7.81	2.38	5.22	1.59
8	2.44	8.92	2.72	5.96	1.82
9	2.74	10.04	3.06	6.71	2.05
10	3.05	11.15	3.40	7.45	2.27
11	3.35	12.27	3.74	8.20	2.50
12	3.66	13.38	4.08	8.94	2.72
13	3.96	14.50	4.42	9.69	2.95
14	4.27	15.61	4.76	10.43	3.18
15	4.57	16.73	5.10	11.18	3.41

3.4   Testing Process for Spalling and Scaling Experiments

The testing process for the measuring of spalling and scaling was different from that used for the cracking. Measurements for spalls and scales are essentially the same, for 3D photogrammetry only calculates the location of the surface. Classifying spalling and scaling with 3D photogrammetry uses the principle that volume is lost from the deck surface.   This measurement can either be calculated as volume or area depending on the value the bridge inspector is looking for.

With the difficulty of replicating pieces of concrete being removed from the surface, real world specimens where used for the experiments. Scales were found in the local sidewalks and concrete floors around the area. Measurements were taken of scaling, but 3D photogrammetry would show the same capability to measure spalling. The depth and width of scales being tested were measured using a ruler to compare to those found from the model. These experiments used a process similar to that of the crack experiment in

the collecting of images. Photos were taken at the height of 2 ft (61 cm) for the first five scaling tests. The final two scaling tests were completed at a distance of 5.5 ft (1.68 m) from the scales to see how the ability to measure scales diminishes with distance.

3.5   *Transferring Data into ArcGIS*

The transfer of the digital elevation model (DEM) into ArcMap, a part of ArcGIS 10 (ESRI Inc. 2010), was performed to enhance the display of information inside the model. By exporting the DEM into ArcMap the user is able to display the model in an easier to visualize format. After some modifications to the DEM, ArcMap allows the user to display the information in several different formats that are useful to a bridge inspector. ArcMap can show the elevations of the model at different gradients that can be defined by the user to display elevation changes. This allows for the measurement of the change in elevation to determine what can be measured using 3D photogrammetry based on elevation.

The first part of this process is to input the data into ArcMap which can be done through the use of the "add data" button. This brings the data into the program as a layer which will show up as a one rectangle, so several different processes have to be completed to display the information properly. A raster calculator function is used to define a temporary raster data set in which all values greater than zero will be set to one from the original raster set. A raster data set is a matrix of cells (or pixels) with values associated with them, in this case 3D coordinates. Layout of this step is shown in Figure 3.8 as the SetNull function is used to complete this process. The next action is to convert the raster into a polygon using the raster to polygon function located in the ArcToolbox under conversion tools. Settings to complete this are shown in Figure 3.9 in which the "simple polygons" option is clicked off. This creates a shapefile of the formed polygon and is used as a masking file. The final step is to extract the mask shapefile that was formed from the original DEM taken from AgiSoft PhotoScan. Figure 3.10 shows how the final process was completed producing a DEM that will correctly display the necessary information in ArcMap.
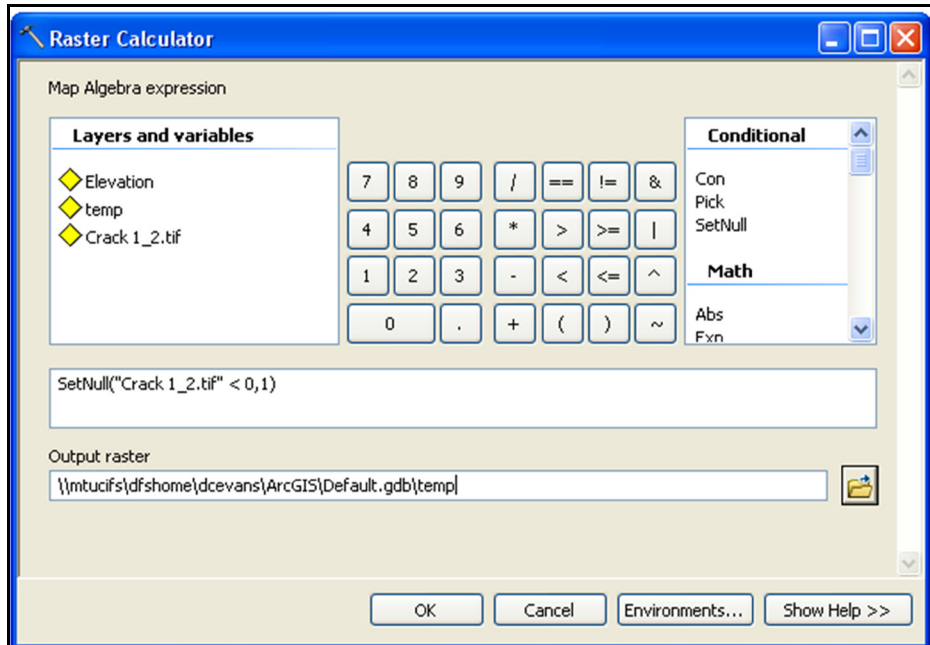
Figure 3.8: Raster Calculator in ArcMap
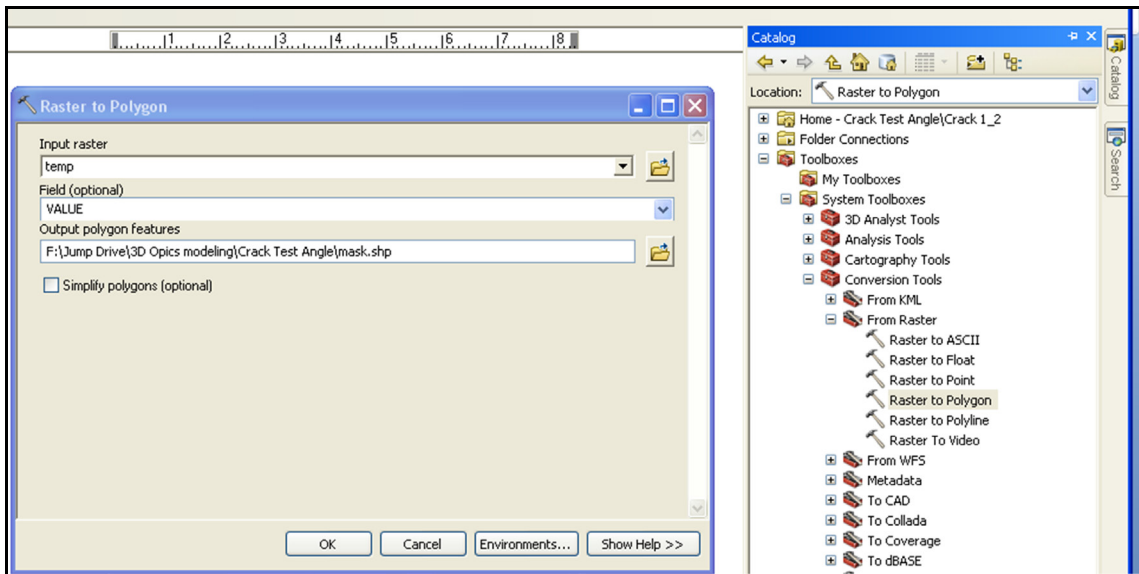
Figure 3.9: Raster to Polygon Conversion in ArcMap
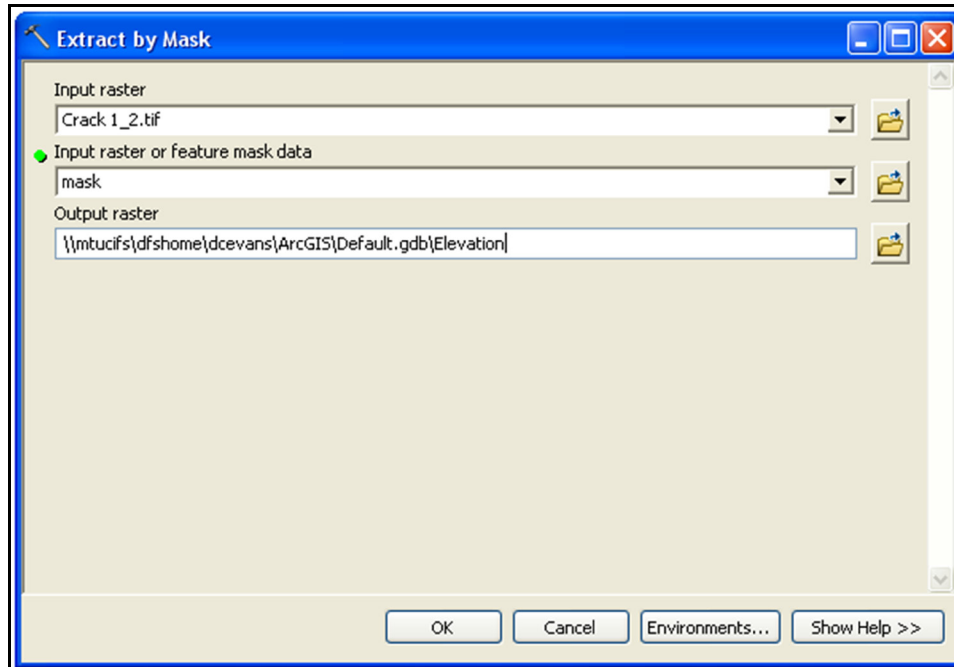
Figure 3.10: Extract by Mask Function in ArcMap

Once the DEM is displayed correctly, the symbology function was used to show the data similarly for all the models. The symbology function has many different options as shown in Figure 3.11. This study used the classified function to allow the same changes in elevation to be measured in each model. Changes in elevation were set for the crack models at 0.079 in. (2 mm) creating a contour map of each model. Figure 3.12 shows how the values for each of the contour gradients were classified. On the right side of the figure the break values can be seen, these were then changed manually. Completing this process allowed for all the models to be normalized for comparison.
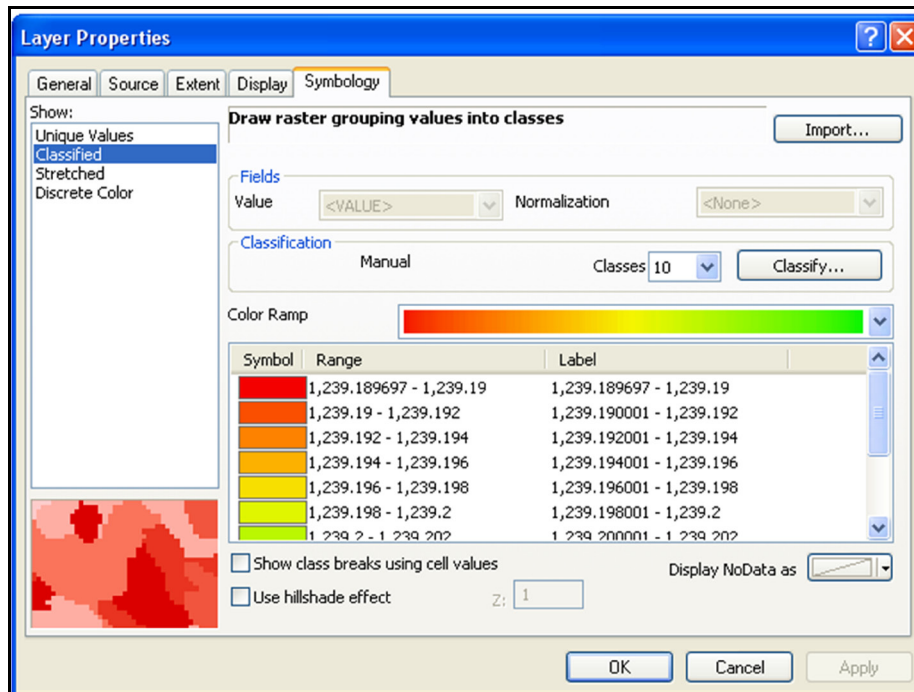
Figure 3.11: Layer Properties in ArcMap
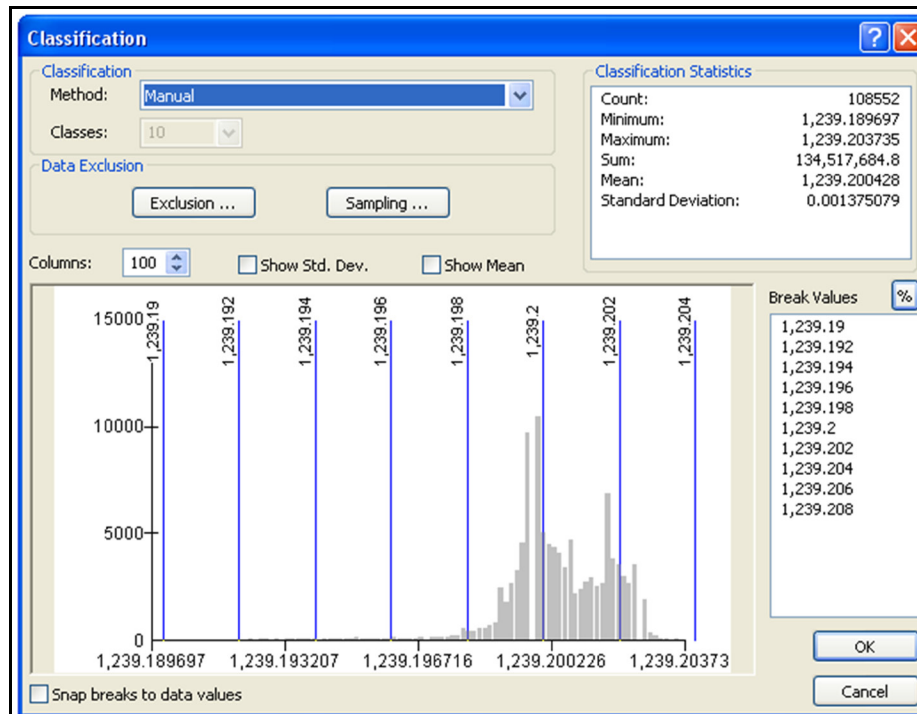
Figure 3.12: Classification Function in ArcMap

To measure the percent or area of scaling or spalling, the number of raster cells at each elevation could be used. Each point has an associated area with it making calculating the area of spalling or scaling possible. Taking the number of raster cells below a certain elevation as the elevation at which would indicate a spall or scale is present and multiplying the number of points times the area of each point will produce the area of scaling or spalling. The percentage of scaling or spalling is as simple as taking the ratio of points below the scaling or spalling elevation to those above that line. An example of raster cells for a model is shown in Figure 3.13. These points can be accessed by looking at the data for the histogram of the model.
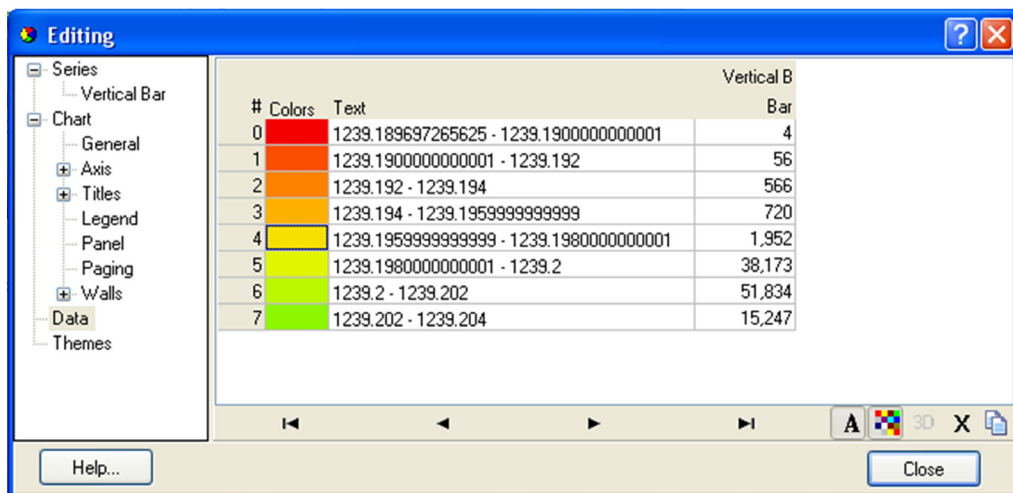
Figure 3.13: Number of Raster Cells at Each Elevation from Histogram

4   Results

4.1   Resolvable Crack Widths in Concrete

The first experiment was conducted with the five photos of each specimen and is shown
in Figure 4.1. Screen shots from PhotoScan of each of the different models were created
for the crack width as a comparison. The view of the models is of the underside of the
surface showing the points below the surface. In Figure 4.1, it can be observed that once
the crack width reached ¼ in. (6.35 mm) the points below the surface become prevalent.
This shows that that ¼ in (6.35 mm) cracks are apparent and that if an algorithm were
created to measure the points differentiating from the deck surface it would pick up the
points in any crack greater than ¼ in (6.35 mm) as long as it is not filled with other
materials.
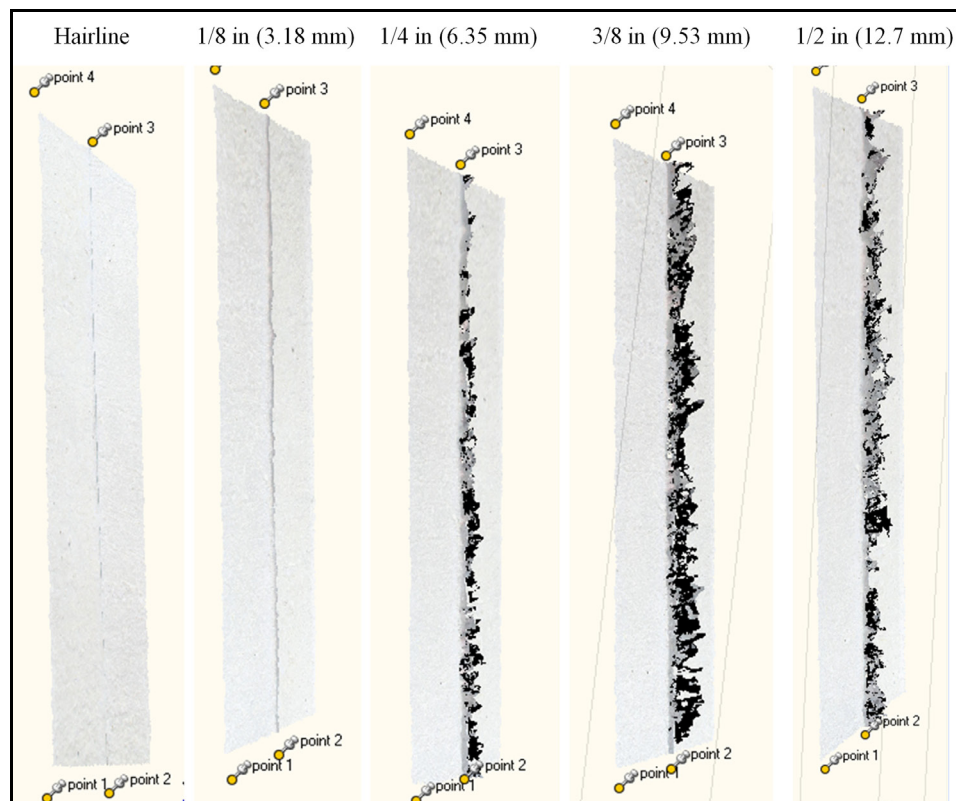
**Figure 4.1: AgiSoft PhotoScan models for the Different Crack Widths with Five
Photos Modeled from Two Feet Away**

Figure 4.2 shows the results from the second experiment conducted which was similar to the first experiment with the difference being fifteen photos used instead of the five. The results from this experiment, as can be seen, are similar to the first experiment which shows that the increase in photos did not lead to increased accuracy based upon the PhotoScan models. More points were created with these models, but appear to offer little or no increased accuracy with these models although there was a decrease in noise. This led to the use of fewer photos in the next experiments to help reduce the amount of processing time for the models.
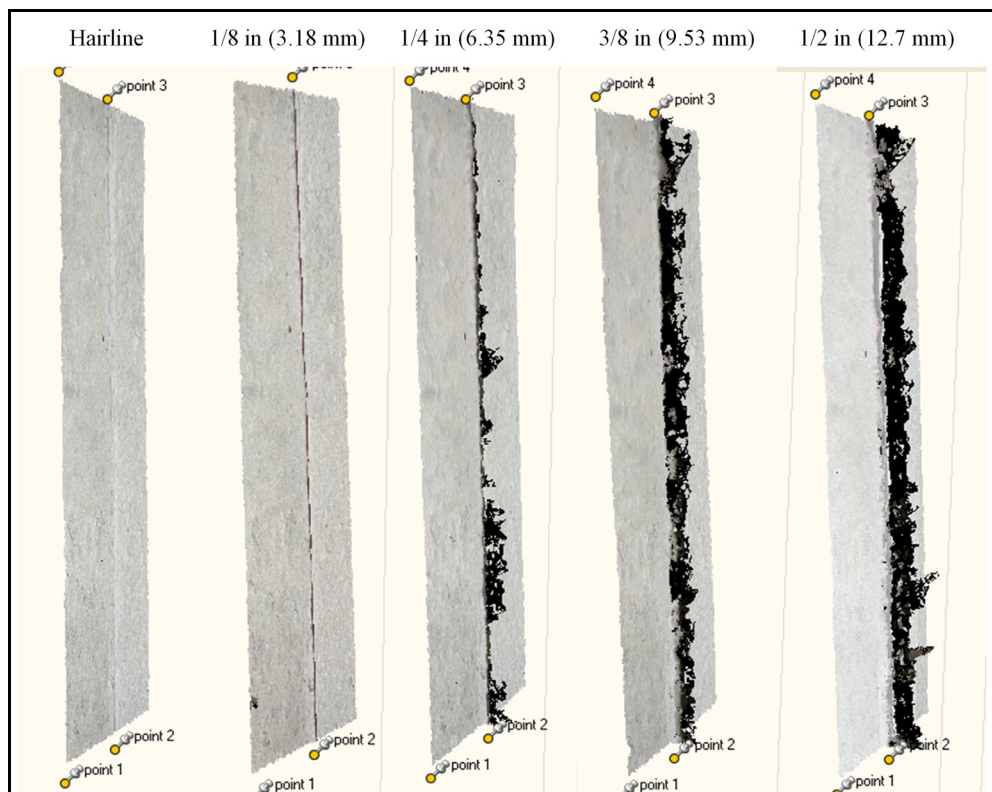
Figure 4.2: AgiSoft PhotoScan models for the Different Crack Widths with Fifteen Photos Modeled from Two Feet Away

Similar experiments were conducted at the other standoff distances using five photos in which the values are shown in Table 4.1. Showing as the distance from the specimen increased, the ability to measure cracks decreased, as expected. The measurements lost about 1/8 in. (3.18 mm) in accuracy for each subsequent standoff distance. This showed

33

that the greater the accuracy required, the closer the camera would have to be to the specimen, or an increase in resolution with a different camera would be required.

Table 4.1:

Crack Width Size Resolved Using AgiSoft PhotoScan

Crack Size Resolved	
Distance ft (m)	Crack Size in (mm)
2 (0.61)	1/4 (6.35)
5.5 (1.68)	3/8 (9.53)
11 (3.35)	1/2 (12.7)

The measurements were then analyzed in ArcMap which allowed for the visualization of elevation differences. Using elevations showed some difference from the results taken from AgiSoft PhotoScan. One difference concluded was that the images from the fifteen photos compared to the five photos seemed to be much clearer as far as definition of the crack area as seen in Figure 4.3. This shows that the model has less noise with more photos, but does not necessarily correlate to greater accuracy due to the increase in points in the model.
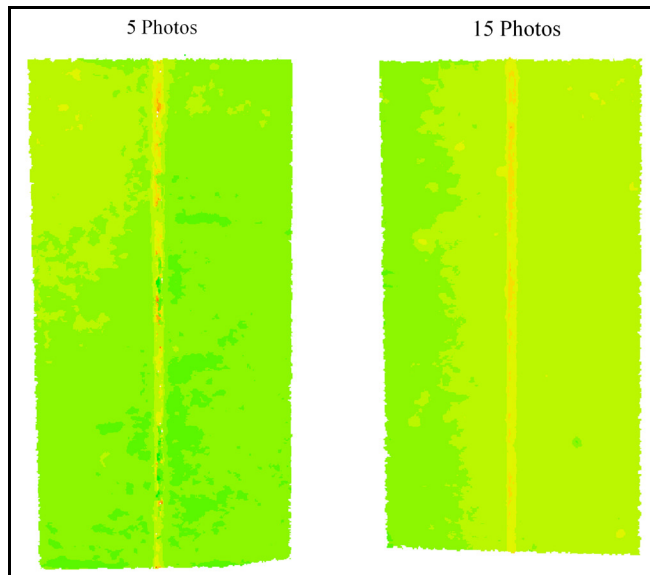
Figure 4.3: Comparison of 5 Photos to 15 Photos using ¼ in. (6.35mm) Crack Specimen in ArcMap

The ability to measure cracks based on the DEM created from the model is based on measuring the change in elevation. DEMs of the five different crack widths at 2 ft (61 cm) away can be seen in Figure 4.4. This shows that a 1/8 in. (3.18 mm) crack could be resolved by the technique using a 0.079 in. (2 mm) elevation change. The slight change in elevation will make transferring this accuracy to the field difficult but does show the capabilities of 3D photogrammetry. DEMs of all the models are available in Appendix A.
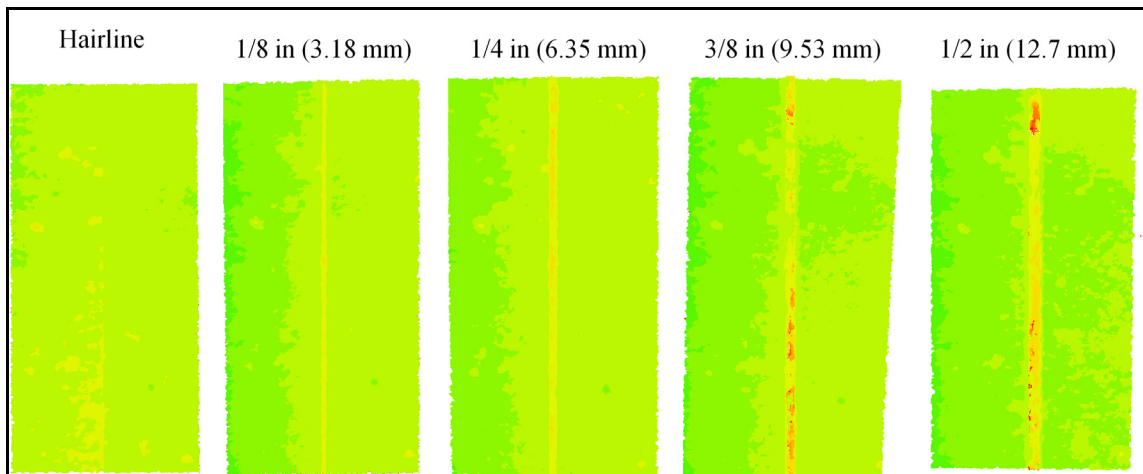
Figure 4.4: Comparison of Cracks at 2 Feet Away

The cracks resolved using DEMs in ArcMap were better than those found using the AgiSoft PhotoScan models. DEM results are shown in Table 4.2 and show the crack widths that were able to be resolved were 1/8 in. better than those taken from the PhotoScan Models (Table 4.2). The use of DEMs to determine crack width size was better than taking the measurements directly from the model. By measuring the change in elevation, allows a less subjective measurement of crack width size that can be resolved. Therefore, it is concluded that the use of DEMs for assessing the ability of 3D photogrammetry is better than taking measurements directly from the PhotoScan models.

Table 4.2:

Crack Width Results Using DEMs in ArcMap

Crack Size Resolved	
Distance ft (m)	Crack Size in (mm)
2 (0.61)	1/8 (3.18)
5.5 (1.68)	1/4 (6.35)
11 (3.35)	3/8 (9.53)

4.2   Resolvable Concrete Spalling and Scaling

Four different scales were examined that consisted of several different sizes and severities in existing concrete specimens. Elevation difference was used to determine the ability to measure whether or not the scales could be resolved. These tests were completed in a similar fashion to those done for cracks with the camera being two feet above the surface. The percentage of spalling or scaling could easily be calculated by knowing the number of raster cells under a certain elevation (i.e. the scaling criteria). This was based on a visual analysis of the models for these tests.

The first scaling test was completed using one of the concrete lab floors and is shown in Figure 4.5. The DEM of the scaling is shown in Figure 4.6, and shows the elevation at 0.079 in. (2 mm) of elevation bands. The elevation model shows four different scales that were in this section of the concrete with the smallest one being about 1 in. (2.54 cm) in diameter on the far left. Based on the elevation changes, the deepest scale was 0.157 in. to 0.236 in. (4 to 6 mm) in depth. The results show that scales in this floor where able to be detected using this technique.

Figure 4.5: Picture of Scales in Test 1
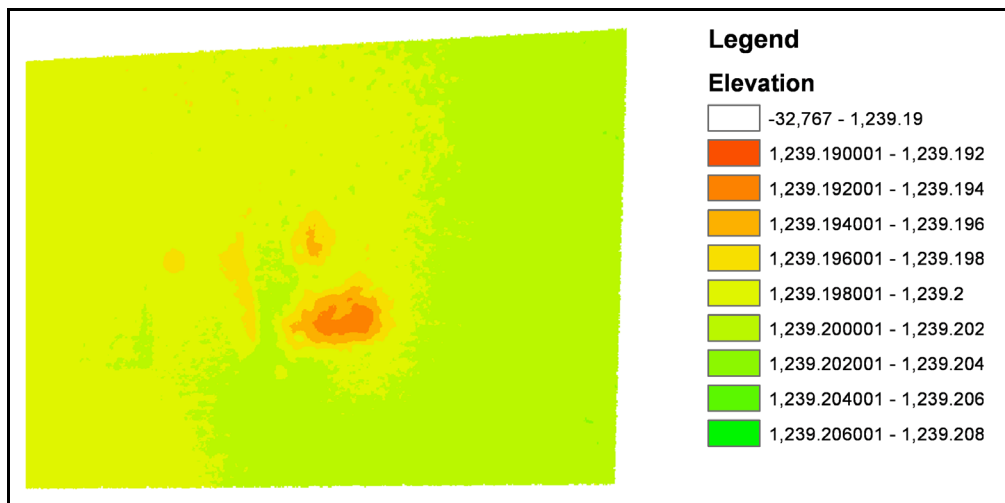
Figure 4.6: Elevation Model of First Scale Test

The percentage of area that is scaled in this model was calculated using the number of raster cells from the histogram data for this model. The data (Figure 4.7) shows all the values at the different elevations. With this data 16,567 raster cells were created that were not part of the surface and had an elevation of -107,503 ft (-32,767 m). The raster cells are shown as clear and are not used for the calculating percentage scaled. For the calculation of percent scaling any elevation below 4062.329 ft (1239.198 m), based upon visual analysis, was used besides the raster cells at -107,503 ft (-32,767 m). The percentage of scaling in this model was 3.4 percent.

#	Colors	Text	Vertical B Bar
0		-32767 - 1239.1900000000001	16,567
1		1239.1900000000001 - 1239.192	0
2		1239.192 - 1239.194	1,219
3		1239.194 - 1239.1959999999999	2,367
4		1239.1959999999999 - 1239.1980000000001	5,822
5		1239.1980000000001 - 1239.2	153,521
6		1239.2 - 1239.202	113,195
7		1239.202 - 1239.204	57

Figure 4.7: Breakdown of Raster Cells at the Different Elevations for Scale Test 1

The results in second experiment considered a smaller single scale which is shown in Figure 4.8. The DEM is shown in Figure 4.9 in which the spall can be seen to have about a 0.157 in. to 0.236 in. (4 to 6 mm) elevation change. This scale was located by itself which made isolating its measurement possible, and as can be seen it was able to be measured using 3D photogrammetry. The percent area of scaling was calculated in this model taking any elevation below 4065.604 ft (1239.196 m) while extracting the raster cells between -107,503 to 4065.558 ft (-32,767 – 1239.182 m). The percent area scaled was 0.64 percent of the area based on the raster cells from the histogram shown in Figure 4.10.

Figure 4.8: Picture of Scale in Test 2

Figure 4.9: Elevation Model for Scale in Test 2

Figure 4.10: Breakdown of Elevation Raster cells for Scale in Test 2

The third test was similar to that of the second test, but with the scaling being smaller than the one in the second test. Figure 4.11 shows a picture of the scale which is in between the ruler and the joint in the sidewalk. The scale was able to be measured as seen in Figure 4.12, but only had an elevation change of about 0.157 in. (4 mm) and had a

0.75 in. (19.1 mm) diameter. This would be on the edge of what will be discernable from that of regular surface roughness.

Figure 4.11: Picture of Scale in Test 3
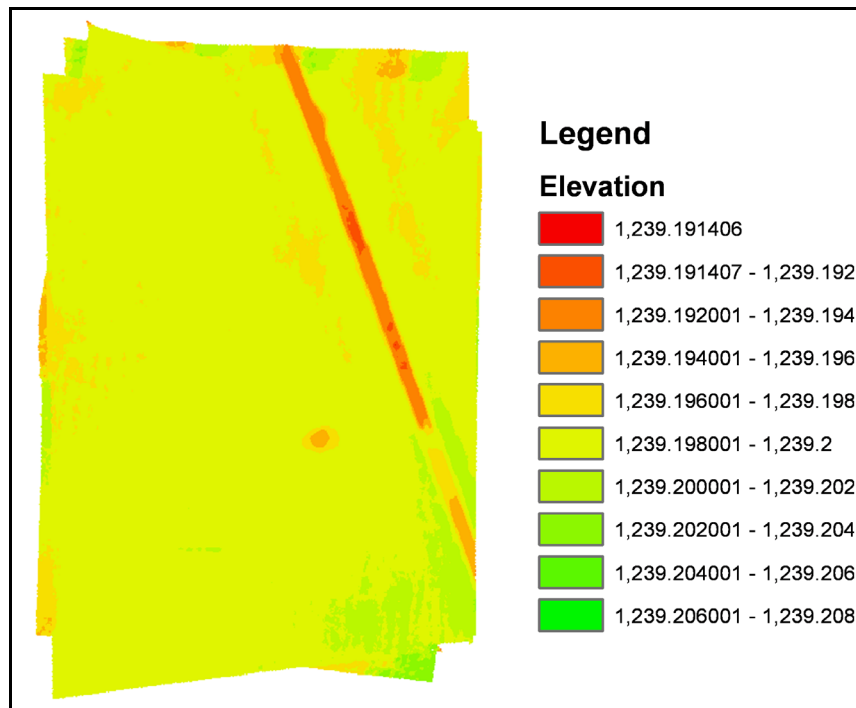
Figure 4.12: Elevation Model for Scale in Test 3

Area of scaling can still be calculated in this model, but includes the area from the joint in the sidewalk. The elevation of 4065.597 ft (1239.194 m) was used as the cut off for scaling as the raster cells were taken out of the histogram in Figure 4.13. The percent area scaled was 1.8 percent, but as can be seen most of the area consisted of the sidewalk joint. This could be one of the issues that would have to be worked out as it will pick up both cracks and joints. This is clearly a concern as 3D photogrammetry and subsequent processing of data will pick up both cracks and joints.

#	Colors	Text	Vertical B Bar
0		1239.19140625 - 1239.19140625	1
1		1239.19140625 - 1239.192	441
2		1239.192 - 1239.194	4,096
3		1239.194 - 1239.1959999999999	3,063
4		1239.1959999999999 - 1239.1980000000001	17,600
5		1239.1980000000001 - 1239.2	209,954
6		1239.2 - 1239.202	13,179
7		1239.202 - 1239.204	950

Figure 4.13: Breakdown of Elevation Raster cells for Scale in Test 3

The fouth test completed was taken of an area with significant scaling to show an area with several scales as can be seen in Figure 4.14. The DEM is shown in Figure 4.15 and several different areas can be seen to be scaled as expected. These scales are not very deep with an elevation change of 0.236 in. to 0.315 in. (6 to 8 mm) of change. To calculate the area of scale in this model, any value below 4062.329 ft (1239.198 m) was taken as a scale using the point information from the histogram in Figure 4.16. This percentage was calculated to be 15.38 percent in this model. This showed an area with a much larger percentage of scaling relative to previous experiments, validating that the technique works for larger areas also.
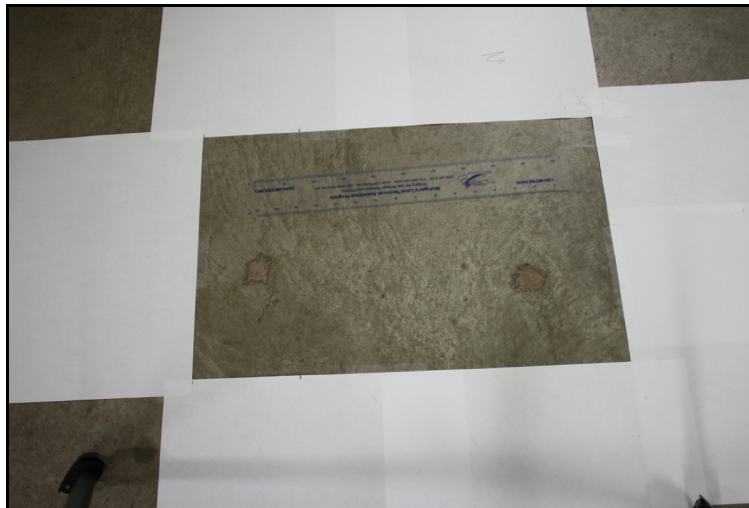
Figure 4.14: Picture of Scaling in Test 4

Legend

■ (red)	-32,767 - 1,239.186
■ (orange-red)	1,239.186001 - 1,239.188
■ (orange)	1,239.188001 - 1,239.19
■ (light orange)	1,239.190001 - 1,239.192
■ (yellow)	1,239.192001 - 1,239.194
■ (yellow-green)	1,239.194001 - 1,239.196
■ (light green)	1,239.196001 - 1,239.198
■ (green)	1,239.198001 - 1,239.2
■ (green)	1,239.200001 - 1,239.202
■ (bright green)	1,239.202001 - 1,239.204
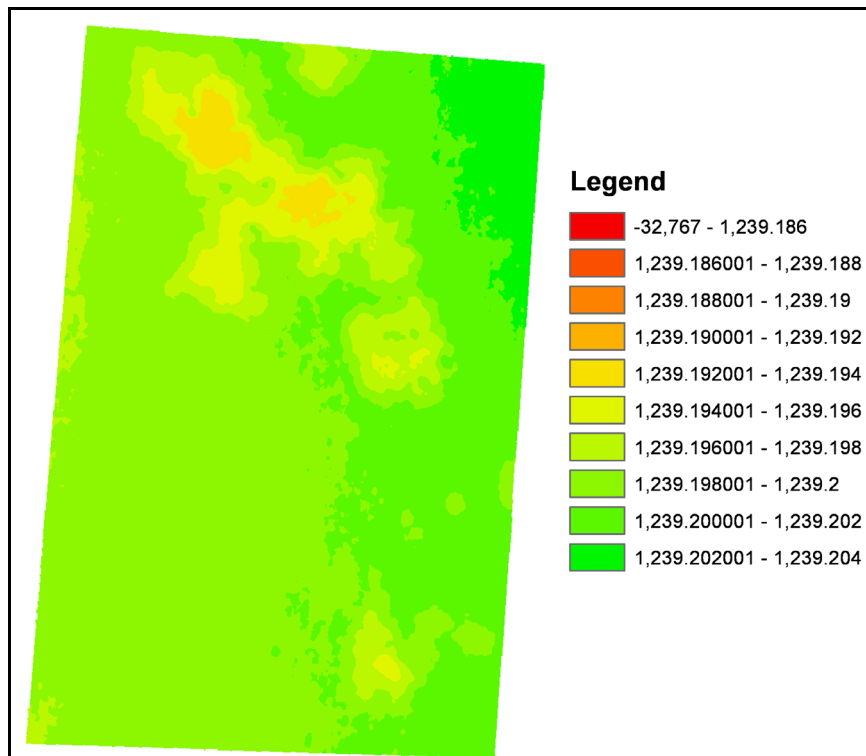
Figure 4.15: Elevation Model of Scaling in Test 4

#	Colors	Text	Vertical B Bar
0		-32767 - 1239.1859999999999	1
1		1239.1859999999999 - 1239.1880000000001	0
2		1239.1880000000001 - 1239.1900000000001	0
3		1239.1900000000001 - 1239.192	0
4		1239.192 - 1239.194	9,121
5		1239.194 - 1239.1959999999999	24,683
6		1239.1959999999999 - 1239.1980000000001	51,682
7		1239.1980000000001 - 1239.2	297,361
8		1239.2 - 1239.202	143,537
9		1239.202 - 1239.204	29,302

Figure 4.16: Breakdown of Elevation Raster Cells for Scaling in Test 4

The fifth scaling test was setup up differently from the first four tests as an area was formed around the scales using paper as seen in Figure 4.17. Allowing the scaling area of the model to be calculated and compared to the actual measured value. For the DEM shown in Figure 4.18 the scales were taken as the raster cells under 3.26 ft (0.994 m). Both scales were visible in the image with the one on the left being 7/8 in. (22.23 mm) in diameter and 1/8 in (3.18 mm) in depth. The scale on the right was 1 in. (25.4 mm) in diameter and ¼ in. (6.35 mm) in depth.

Figure 4.17: Picture of Scale Test 5
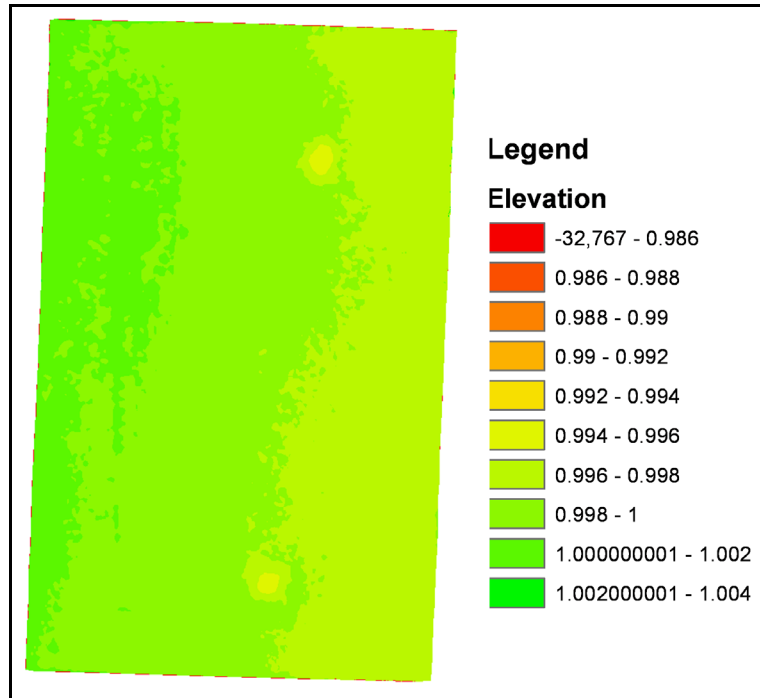
Figure 4.18: Elevation Model of Scaling in Test 5

Area of a rectangle for the model was 10 in. (25.4 cm) by 16 in. (40.64 cm) for an overall area of 160 in^2 (1032.26 cm^2). The area of the two scales in test five had a combined area of 1.23 in^2 (7.94 cm^2) making for an overall percent scaling of the area 0.76 percent. This was compared to the 0.33 percent taken from the raster cells from the model which are shown in Figure 4.19.

Figure 4.19: Breakdown of Elevation Raster cells for Scaling in Test 5

44

Scaling test six consisted of looking at the same scaled section as in test five, but at a standoff distance of 5.5 ft (1.68 m) instead of the 2 ft (61 cm). The DEM is shown in Figure 4.20 and shows that the spalls were unable to be resolved at this distance from the scales.
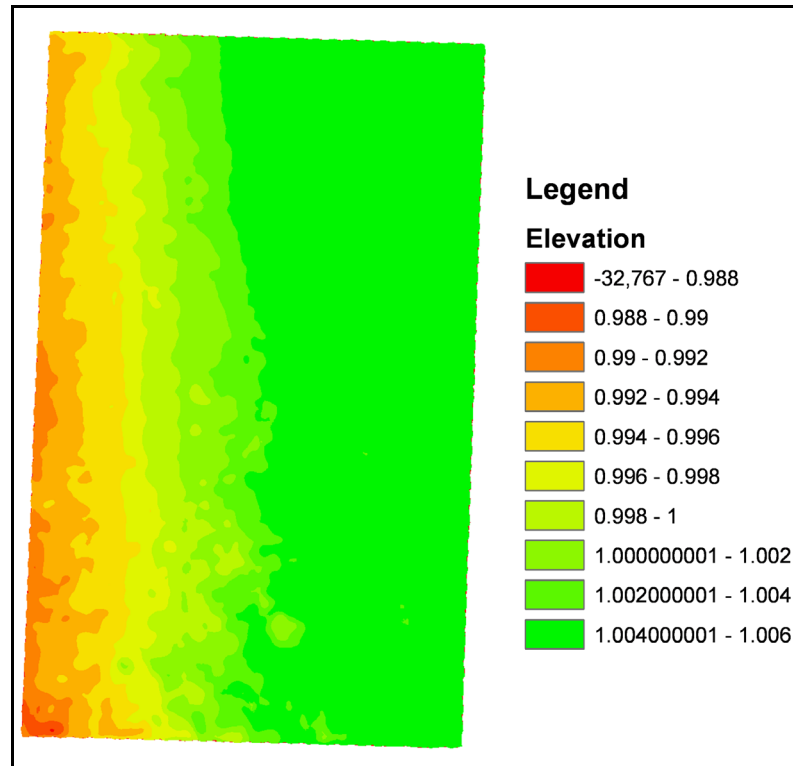
Figure 4.20: Elevation Model of Scaling in Test 6

The final scaling test was done for the same scales as those in the first scale test shown in Figure 4.5. The scale on the bottom right was 1.5 in. (3.81 cm) in diameter and ¼ in. (6.35 mm) in depth as seen in Figure 4.21. With the difference being the standoff distance was 5.5 ft (1.68 m) from the scales. The scales in this case were any elevation below 3.26 ft (0.994 m) for the whole model where local scaling could be considered on the top center of the model below 3.27 ft (0.996 m) as seen in Figure 4.21. The percentage of scaling was 0.18 percent based on the raster cells from Figure 4.22.
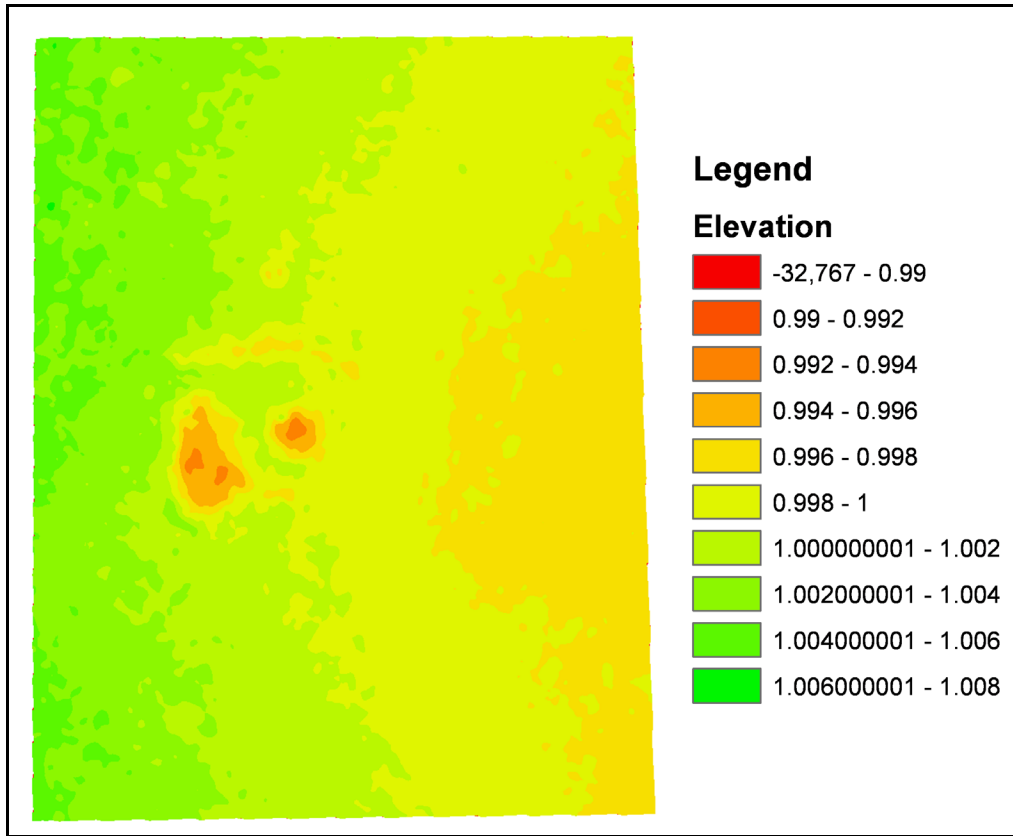
Figure 4.21: Elevation Model of Scaling in Test 7

Figure 4.22: Breakdown of Elevation Raster cells for Scaling in Test 7

46

4.3   Influence of Camera Angle on Measurements

The angle of the camera has the potential to influence 3D photogrammetry and was tested to see how it would affect the ability for measuring surface deterioration mechanisms. Previously noted tests were conducted at a camera angle of 90 degrees to the specimen surface Figure 4.23 shows the comparison of DEMs generated using photos taken perpendicular (90 degrees) to the surface along with photos taken at 45 degrees to the surface. It can be seen that in the perpendicular DEM the ¼ in. (6.35 mm) crack is able to be resolved while with the 45 degree camera angle the crack was not able to be resolved, confirming what the AgiSoft PhotoScan user manual stated in that it was best to take the pictures perpendicular to the surface than at an angle. This was completed with the camera moving perpendicular to the crack along the x-y plane, which would be the surface of the specimen, which could have made seeing the crack more difficult than if the camera was moved parallel along the x-y plane, but cracks can be in any direction. The smallest crack detectable using an angle of 45 degrees was ½ in. (12.7 mm) crack at 2 ft (61 cm) away which is considerable worse than 1/8 in. (6.35 mm) using parallel images. This makes using an angled camera not a good alternative to one perpendicular to the surface. The DEMs of all the crack widths are included in Appendix A.
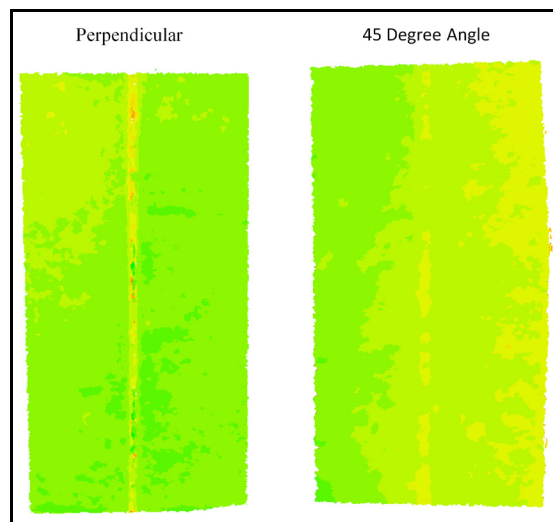
Figure 4.23: Comparison between Different Camera Angles for ¼ in. (6.35 mm) Crack

5 Conclusions

The bridge inspection industry has yet to utilize a rapidly growing technology that shows promise to help improve the inspection process. This work investigated the abilities that 3D photogrammetry could provide to the bridge inspector for a number of deterioration mechanisms. The technology primarily focused on the ability to measure surface defects of a concrete bridge which include cracking, spalling and scaling. Testing was completed using a Canon EOS 7D camera which then processed photos using AgiSoft PhotoScan to align the photos and develop models. Further processing of the models was completed using ArcMap in the ArcGIS 10 program to view the digital elevation models of the surface. Different camera factors including the distance from the defects, number of photos and angle, were also investigated to see how each factor affected the capabilities.

5.1 *Detectable Bridge Deck Deterioration Mechanisms*

Crack width was determined based on the experiments conducted with the camera at various distances from the specimen, as seen in Table 4.1 using AgiSoft PhotoScan. Table 4.2 shows the values for crack width determined using ArcMap to view the DEMs which showed an improvement of about 1/8 in. (3.18 mm) for all the distances over those which can be seen in the PhotoScan models. One of the results that can be derived from these tables is that as the distance away from the surface increases, the resolution of the technique decreases, which would be expected. The crack width that can be resolved does not necessarily correlate to the resolution of the camera, or to the accuracy of the software, but is a combination of the two along with the distance from the object. The smallest cracks using 3D photogrammetry that were able to be determined using the EOS Canon 7D with a 20 mm lens was 1/8 in. (3.18 mm) cracks at a standoff distance of 2 ft (61 cm) and 3/8 in. (9.53 mm) cracks were measured at a distance of 11 ft (3.35 m). These values were determined based on visual analysis of the cracks using the DEMs viewed in ArcMap.

The cracks considered in this experiment were free of any extra material, allowing for points below the surface to be formed. This could affect the expected accuracy in the field, as cracks are typically filled with material on actual bridge decks. A relatively

large number of points in a line below the deck surface were required for the technique to resolve cracks. Therefore, it can be concluded that other methods may be better for crack data collection on a bridge deck. Cracks can be resolved using this technique, but not to the extent that would be required for bridge inspection. One technology that has shown promise in the literature is the use of gray scale for the detection of cracks. This technique works based on the principle that cracks are typically darker than the surrounding surface. Material inside the cracks is not an issue for this technology, as it only considers color and area, instead of 3D coordinates.

The scale measured in the third test had a depth of about 0.188 in. (4.76 mm) and was 0.75 in. (19.1 mm) in diameter and the fifth test had a scale 1/8 in (3.18 mm) in depth and 7/8 in. (22.23 mm) in diameter. These were the smallest scales that would be seen and remain discernable from the area around it using 3D photogrammetry from a distance of two feet. The smallest scale that was able to be resolved from a standoff distance of 5.5 ft (1.68 m) was 1.5 in. (3.81 cm) in diameter and ¼ in. (6.35 mm) in depth from scale test seven. The scales from test six were not able to be measured making for a limit of what cannot be measured, so the limit on what size scale that can be measured from a standoff distance of 5.5 ft (1.68 m) is between a 1.5 in. (3.81 cm) and 1 in. (2.54 cm) diameter scale with ¼ in. (6.35 mm) depth. Approximately the minimum size that a bridge inspector would consider when making a bridge inspection making this a viable technique from within 5.5 ft (1.68 m) from the scaling or spalling based on equipment used for this study.

The percent scaling calculated in test five was compared to the actual measured percentage which was double the area of scaling picked up with the 3D photogrammetry. Several reasons for this discrepancy could be the low percentage of scaling made to the calculation off, or the second is the technique only picks up the scale once a certain elevation change is met so the outside edge of the scale is not measured. Meeting the minimum size standards makes this technique a good option for the bridge inspectors to use for calculating the area or percentage of scaling or spalling as the measurements

should converge as larger areas are considered over the small percentage considered in this study.

5.2 Pros and Cons of the Modeling Software

Based on the performance of the PhotoScan software, several conclusions could be obtained for applications of this software in bridge deck surfaces. This program was designed fairly simply in terms of operations that could be performed. Providing limits on available user options that can be completed by the program was helpful as the features allowed the user to perform the necessary operations for creating a model while not being distracted by added non-essential features for the modeling process. A lower number of features inside the program facilitate the learning process and helped the user understand the program. Increased features for processing the models could have improved the program for this application.

Some advantages of the software are that photos could be uploaded easily and that the automatic recognition system allowed the user to align the photos with no effort, saving time. This type of system would have to be investigated for reliability in the future, as this can possibly create mistakes if the images have no recognizable points that the program can identify. The masking system within the program was a nice feature for this research, as it allowed the program to concentrate on the area being examined in the experiment. Masking allowed for much faster computing times for the models, as all the computing power was focused on the area of concern, instead of all the background objects. Some time was required to go through each of the photos and mask them, but generally saved time in the computer processing portion. The program was able to process the photos into a model easily with a couple inputs chosen by the user to make the best model for the application.

The program interface could have been designed better for the applications required by this project. After the model was created, there was only one point about which the model was allowed to rotate and zoom into the model, limiting the views available while

working in 3D. Working with flat planes, the program could generate, did not allow the model to be viewed in some directions which would have been helpful for this application. The process of setting up a coordinate system inside the model was time consuming, but could have been due to the technology rather than with the actual program. Once the coordinate system was completed, the tool inside the program for making measurements could have been easier to use by not having to place points at each end of what was being measured.

Recommendations for improving the PhotoScan software for the use with bridge inspection would be mostly with the interface of the program processing of the models. Providing multiple views of the finished model would improve the ability to draw conclusions from the model inside of PhotoScan allowing the user to look at the surface along the different planes. Improving the zoom function inside the program would also help with the processing of the model inside the software. With developing a coordinate system for images being processed would be to include an object of know coordinates in the system, so the same keypoint file can be used for all the models. The ability to select one point and directly select another point and get the distance between them would be a useful addition to the program for this application.

5.3   Implementation of 3D Photogrammetry for Bridge Inspections

The implementation of the 3D photogrammetry will be important for applying this technology in the bridge inspection field. This application could have a couple different possible implementation strategies. A bridge inspector would take photos of the area to be modeled with a portable camera. Alternately, a system could be mounted on a vehicle to be moved across the bridge at a constant rate gathering photos of the entire bridge deck. Each application has its benefits and shortcomings in the bridge inspection field.

Having the bridge inspector take the photos and develop a model of the bridge would allow the inspector to ensure that the proper areas are modeled to the accuracy required for an assessment. Bridge inspectors would be allowed the option to model girders or the

underside of the bridge deck, as opposed to just the top of the bridge deck. The bridge inspector would be able to measure the amount of material missing from an area under the bridge without actually going and physically measuring that particular defect. This could be performed by the inspector on a case by case basis, limiting the amount of unnecessary modeling of bridges that are in good condition. This could also be deployed with little actual cost to the agency completing the inspection, because it requires a limited amount of resources to implement.

For the bridge inspector creating the models there are several down sides that could limit the use of 3D photogrammetry. Taking photos could be time consuming for the inspector. In addition to performing their other required duties, taking photos would only add to the inspection time making it less desirable. With the modeling program used in this study, it would also be required that the inspector know coordinates on the area being modeled to be able to gain accurate measurements from the model. This can be accomplished by placing an object of known dimensions on the area being modeled; however, this would be difficult on the underside of a bridge. Another area of concern with this approach would be the time requirement by the inspector to run the model back at the office after the inspection was performed. Adding work for the inspector might make it difficult for this technology to be accepted by the bridge inspection community.

The second application would be to mount the camera on a vehicle. The area over which the vehicle was driven would be able to be modeled through the use of 3D photogrammetry. This process could be automated to configure the photos based on the location at which they were taken. Creating a model of the entire bridge deck surface allows for several different processing options, including manual, spalling or scaling area, spalling or scaling volume or a roughness coefficient. The manual processing of the model would require the inspector to look for defects in the computer model and determine the condition based on their experience. Calculating the spalling or scaling area or volume automatically could be completed by assuming that any point that is more than a certain distance below the flat plane would be considered a spall or scale. The area or volume of these points could then be automatically calculated using an algorithm

developed for this process. The final processing option would be measuring how much the points differ from the average and correlating this to a roughness value. This could possibly be associated to something like IRI values used to calculate the roughness of pavements.

Several issues will have to be considered and worked out if this type of application is to be applied in actual practice. The first part to be considered in a vehicle mounted system is taking photos. Height and number of cameras would have to be determined to provide the necessary coverage and accuracy to assess the condition of the bridge deck. There could be a wide variety of options given all the different types of cameras and lenses available. The cameras would also have to be protected in some way while traveling to and from the collection sites. Protection for the cameras would also possibly have to be permanent if the collection is being done at near highway speeds. The speed at which the vehicle is traveling could also affect the quality of the photos, as blurry images will not be processed or be accurate. Traveling at an exact speed can be difficult, so the cameras may have to be designed to account for the speed of the vehicle. Global positioning system (GPS) could possibly provide a solution to tag the photos so the position of each photo would be known.

There will also be difficulty in determining how to best develop an algorithm for which the roughness or overall spalling or scaling on the bridge deck would be calculated. Issues exist with how this can best be accomplished. The difference in height which is used to consider something as a deterioration mechanism and how to best transpose a surface to the model will have to be worked out. Once this is accomplished, the percentage of deterioration which correlates to the typical bridge deck ratings will have to be discussed. The format in which the data would be displayed and whether or not a model can be completed without the aid of the user making some decisions must be determined.

The benefits of a vehicle mounted system are that a large number of bridges could be documented within a relatively short amount of time. This would allow a more frequent

period of inspection of the bridge deck than is typical. Information could possibly be automatically formatted for the inspector to view as needed for the determination of bridge deck condition. A vehicle mounted system allows for safer collection of data as an inspector does not have to be on the bridge deck and could possibly allow for collection of data, without slowing the traffic in any way. If the automatic processing of the data through algorithms was implemented, a possible warning flag system could be implemented to alert the inspector if a bridge deck has gone below a certain threshold.

The disadvantages to such a system include significant cost as multiple cameras could be required to perform the data collection, in addition to a vehicle designed for this type of collection. If this were completed outside of a normal bridge inspection period, more personnel may have to be hired to carry out the collection of data. The application could be limited by weather, and would have to be scheduled to avoid any weather that would interrupt the picture taking process. This will be a complex process at the start to make sure everything is working the way it is designed to. Difficulty with establishing this as a reliable technique with the bridge inspectors may also limit its applicability in the field.

Recommendations for implementing a vehicle mounted system would be to have several cheaper cameras placed closer to the surface instead of one more expensive camera placed farther away from the surface. The more overlap between the images the better the ability to measure deterioration mechanisms will be. With the camera used in this study, the use of two cameras at 5.5 ft (1.68 m) would be better than placing one camera at 11 ft (3.35 m) as the desired accuracy for scaling and spalling could be achieved. Limiting the height of the cameras would also help improve the portability of the system, but this could decrease if cameras are required to be outside the profile of the vehicle.

6   Future Work

Some of the parameters which could affect the accuracy of the 3D photogrammetry still need to be considered in future work, as they will determine different considerations for implementing this technique. Further work on how the angle would affect the results should be completed to see how far from perpendicular the camera can get before significantly affecting the results. One concern in determining the capabilities of 3D photogrammetry will be lighting conditions, which come in different variations. First would be the ambient light conditions, and whether having less light available decreases the accuracy of the technique. The other situation would be if using the flash would affect the accuracy in particular when examining the underside of a bridge. These areas are typically locations with poor light conditions, making a flash a requirement in some cases. Different weather conditions should be examined to see how this would affect the technology. Including wet pavement as this could change the reflectivity of the surface or fill the defects with water, creating different measurements.

Other work that will be required with 3D photogrammetry will be to develop exact parameters for measuring the roughness of the surface. This could possibly be accomplished through a statistical analysis of deviation from a plane, which in this case, would be the roadway surface. Roughness measurements could become a more useful assessment of a bridge deck as the roughness becomes more measureable with this technique compared to current techniques. 3D photogrammetry could prove better than any previous roughness assessment technique, as this technique is unaffected by a vehicle moving up and down. The key will be establishing limits for how much roughness will correlate to a certain rating, or how bridge inspectors will be able to successfully use this data.

A computer processing algorithm will have to be developed to account for slopes on the bridge deck. All bridge decks are sloped to some degree to allow for drainage, and will make the processing difficult when considering a flat plane analysis. Whether this is taken into account in the computer processing or from the angle of the vehicle when it is

taking the photos will have to be determined before 3D photogrammetry assessment using a vehicle will be successful.

The next important step to determine the capabilities of 3D photogrammetry will be deploying the technique in the field. This will help demonstrate to the bridge inspectors that 3D photogrammetry could be a useful inspection tool. Field testing will allow real world results to be obtained for the bridge inspection field. Even if this technology has to be developed further to actually implement it, field testing could demonstrate its capabilities to bridge inspectors. 3D photogrammetry should eventually prove to be an efficient technique in assessing bridge deck conditions.

7   References

AgiSoft LLC. 2010. AgiSoft PhotoScan, Professional Edition. Version 7.0.

American Association of State Highway and Transportation Officials (AASHTO). 2008.
     The Manual for Bridge Evaluation. Washington D.C.: American Association of
     State Highway and Transportation Officials.

Armesto J, Arias P, Roca J and Lorenzo H 2008. Montoring and Assessing Structural
     Damage in Historic Buildings. The Photogrammetric Record 23(121):36-50.

Benning W, Lange J, Schwermann R, Effkemann C and Görtz S. Monitoring Crack
     Origin and Evolution at Concrete Elements using Photogrammetry. XX ISPRS
     Congress; 2004; Istanbul, Turkey: International Society for Photogrmmetry and
     Remote Sensing.

Chung T, Carter C, Masliwec T and Manning D 1994. Impulse Radar Evaluation of
     Concrete, Asphalt and Waterproofing Membrane. IEEE Transactions on
     Aerospace and Electronic Systems. 30(2):404 - 415.

Edin H 2006. Field Of View Calculator [Internet]. [Last Accessed March 8, 2011].
     Available from: http://www.howardedin.com/articles/fov.html

ESRI Inc. 2010. ArcGIS 10. Redlands, CA.

Federal Highway Administration (FHWA). 2010. Deficient Bridges by State and
     Highway System [Internet]. United States Department of Transportation. [Last
     Accessed January 15, 2011]. Available from:
     http://www.fhwa.dot.gov/bridge/deficient.cfm

Federal Highway Adminstration (FHWA). 2006. Bridge Inspector's Reference Manual
     (BIRM). Washington, D.C.

Furuta H, Hattori H and Frangopol D 2006. Damage Assessment of Reinforced Concrete Bridge Decks using TAM Network. Advances in Engineering Structures, Mechanics & Construction:81–86.

Gastineau A, Johnson T and Schultz A 2009. Health Monitoring and Inspection - A Survey of Methods. Department of Civil Engineering University of Minnesota.

Gillespie T 1992. Everything You Always Wanted to Know about the IRI, But Were Afraid to Ask!,. The University of Michigan Transportation Research Institute.

Gruen A and Akca D 2005. Least Squares 3D Surface and Curve Matching. Journal of Photogrammetry & Remote Sensing 59:151– 174.

Ito A, Aoki Y and Hashimoto S Accurate Extraction and Measurement of Fine Cracks from Concrete Block Surface Image. Waseda University and Shibaura Institute of Technology.

Jiang R, Jauregui D and White K 2008. Close-Range Photogrammetry Applications in Bridge Measurement: Literature Review. Measurement 41:823–834.

Maas H and Hampel U 2006. Photogrammetric Techniques in Civil Engineering Material Testing and Structure Monitoring. Photogrammetric Engineering & Remote Sensing 72(1):39-45.

National Cooperative Highway Research Program (NCHRP). 2007. Bridge Inspection Practices - NCHRP Synthesis 375. Washington DC: Transportation Research Board.

Nowak A, Szerszen M and Juntunen D 2000. Michigan Deck Evaluation Guide. In: Construction & Technology Division, editor. Lansing, MI.

Pankow M, Justusson B and Waas A 2010. Three-Dimensional Digital Image Correlation Technique using Single High-Speed Camera for Measuring Large Out-of-Plane Displacements at High Framing Rates. Applied Optics. 49(17).

Reay S, Appleyard M, Van Dam T and Sandberg L 1998. Sealing and Filling of Cracks for Bituminous Concrete Pavements. Michigan Technological University.

Scheff J, Chen J and Roger H Bridge Decks Inspection Using Chain Drag and Ground Penetrating Radar. In: Farhad A., editor. 2000: American Society of Civil Engineers. p. 13.

Sohn H, Lim Y, Yun K and Kim G 2005. Monitoring Crack Changes in Concrete Structures. Computer-Aided Civil and Infrastructure Engineering 20:52–61.

Xu B and Huang Y 2003. Automated Pavement Cracking Rating System: A Summary. Center for Transportation Research The University of Texas at Austin.

Yilmaz H, Yakar M and Yildiz F 2008. Digital Photogrammetry in Obtaining of 3D Model Data of Irregular Small Objects. Remote Sensing and Spatial Information Sciences XXXVII(Part B3b):125-130.

Appendix A
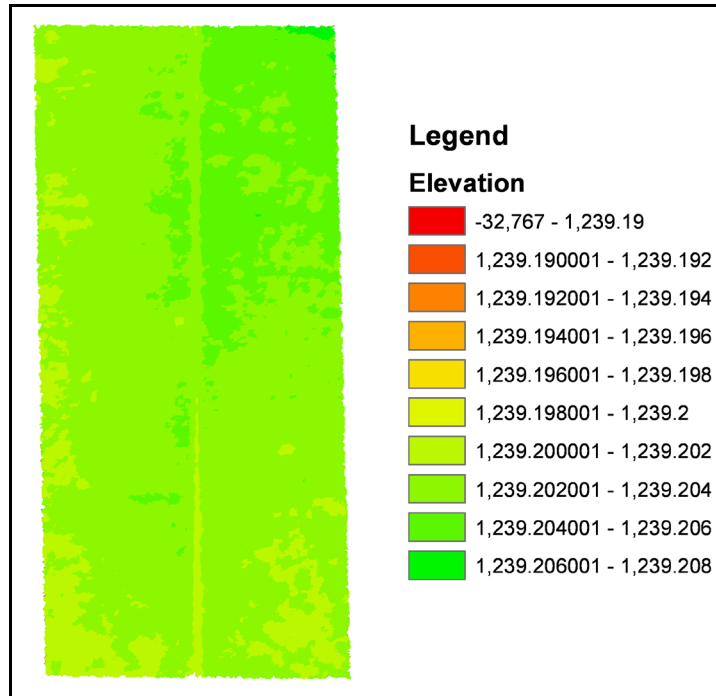
Figure A.1: DEM of Hairline Crack at 2 ft (61 cm) away using 5 Photos Displayed in ArcGIS
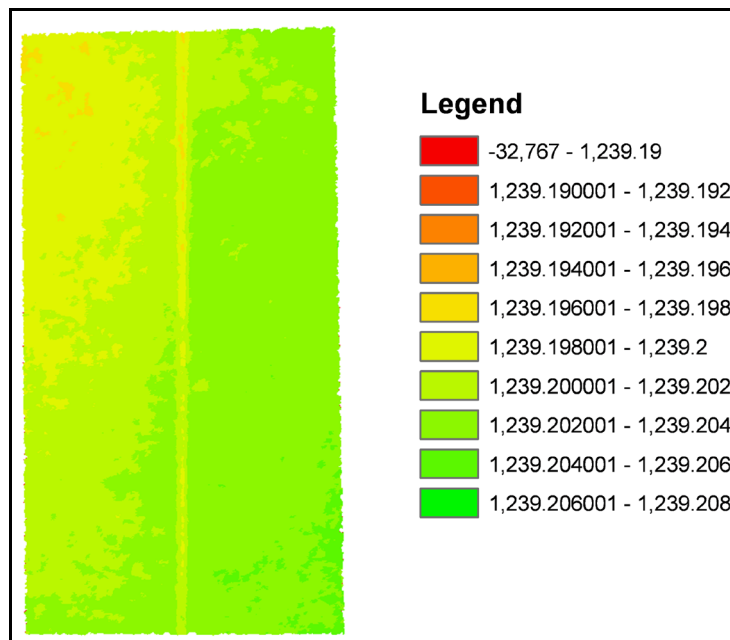
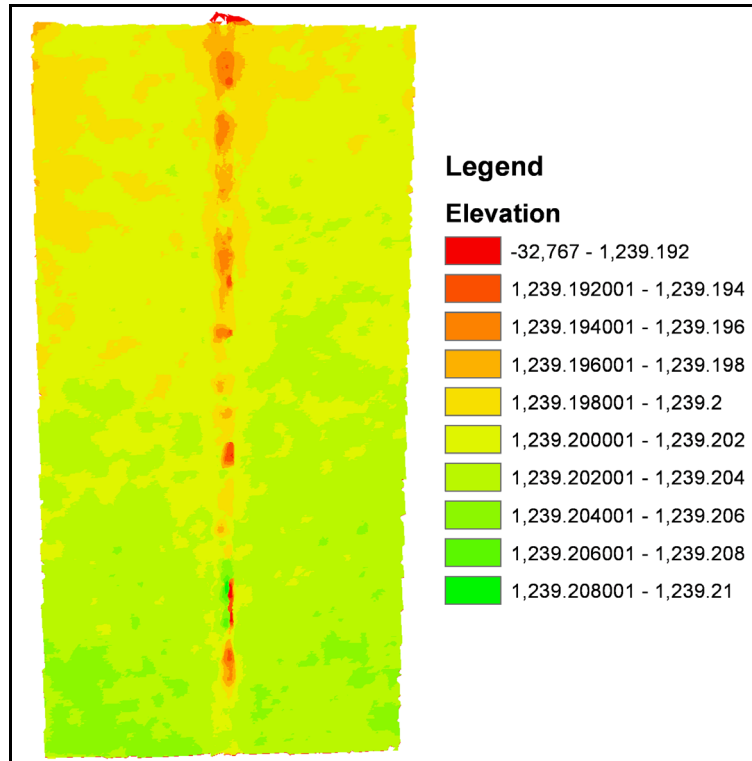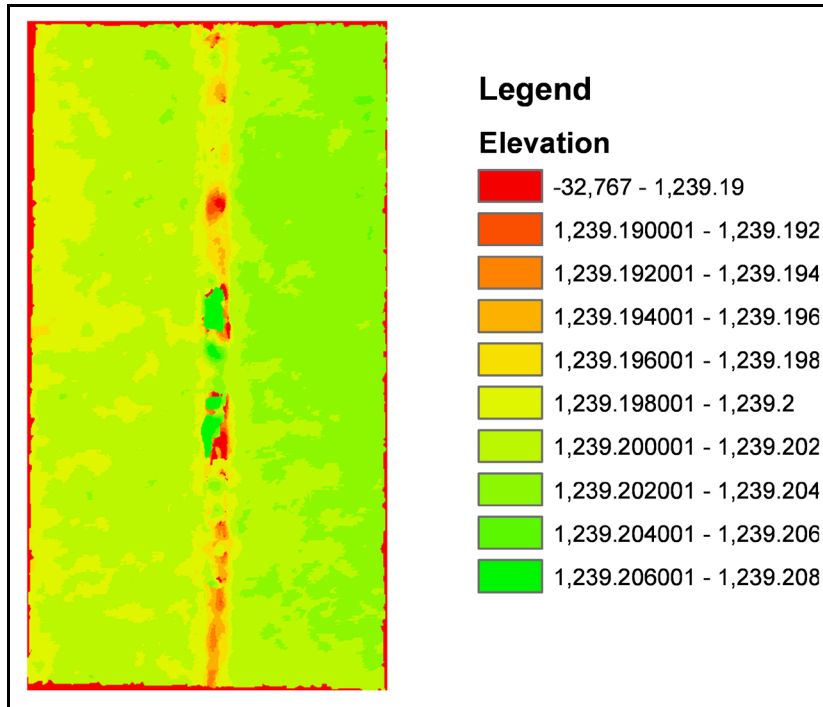**Figure A.2: DEM of 1/8 in. (3.18 mm) Crack at 2 ft (61 cm) away using 5 Photos Displayed in ArcGIS**
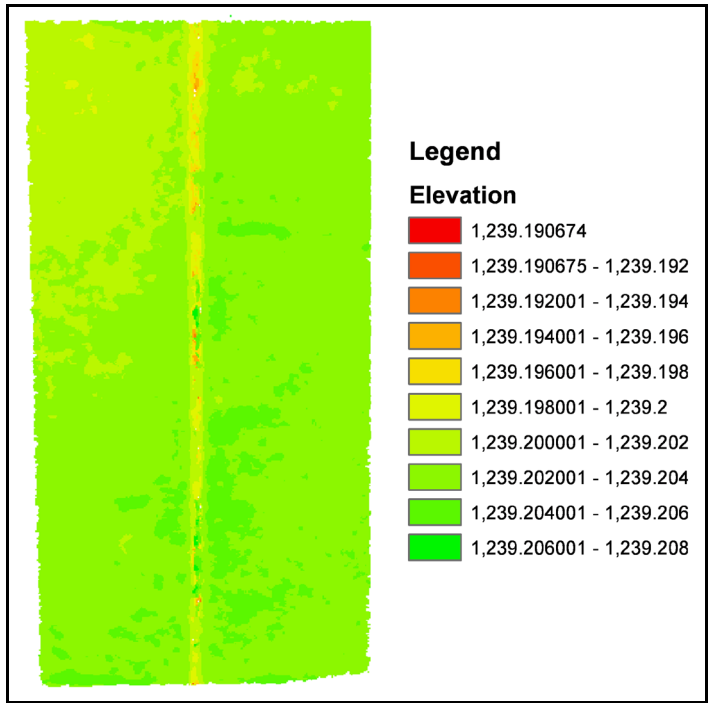
Figure A.3: DEM of ¼ in. (6.35 mm) Crack at 2 ft (61 cm) away using 5 Photos Displayed in ArcGIS
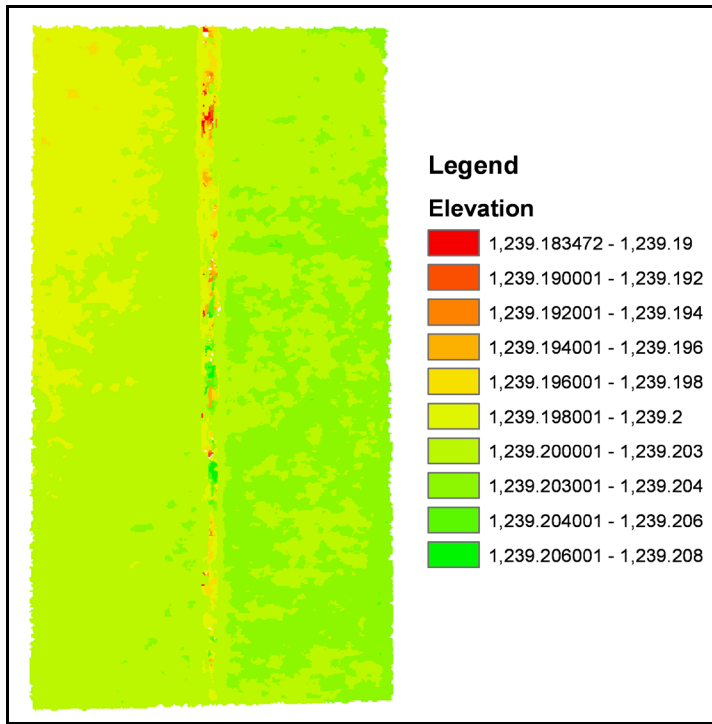

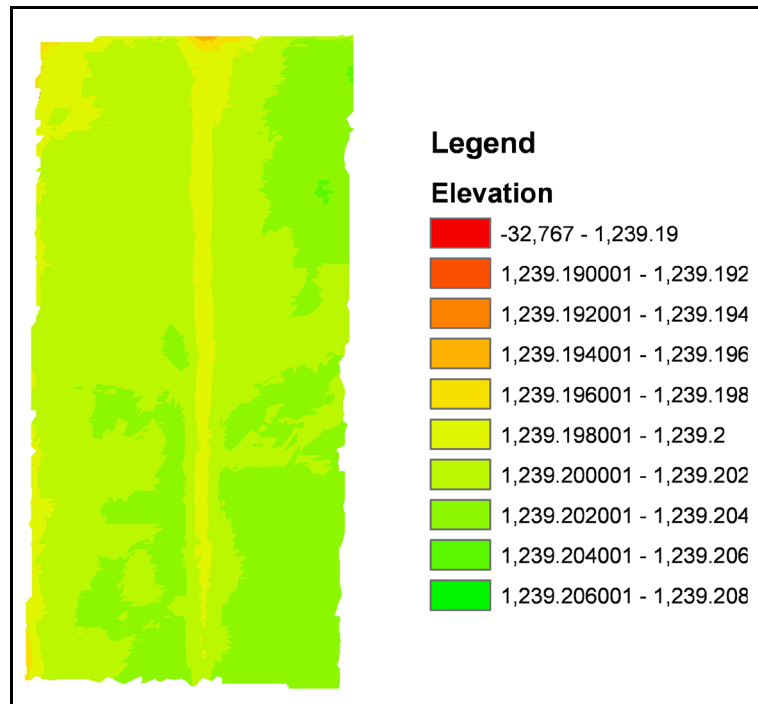**Figure A.4: DEM of 3/8 in. (9.35 mm) Crack at 2 ft (61 cm) away using 5 Photos Displayed in ArcGIS**
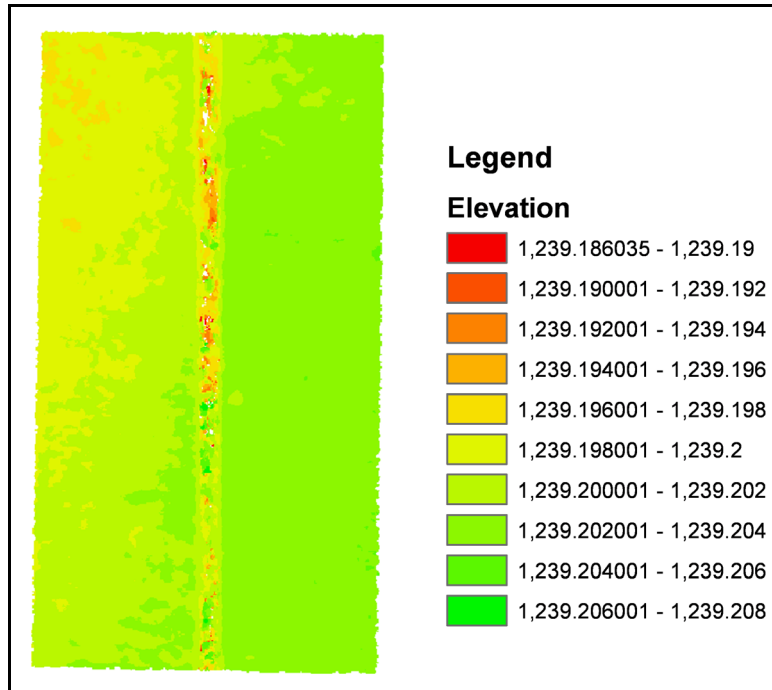
Figure A.5: DEM of ½ in. (12.7 mm) Crack at 2 ft away using 5 Photos Displayed in ArcGIS
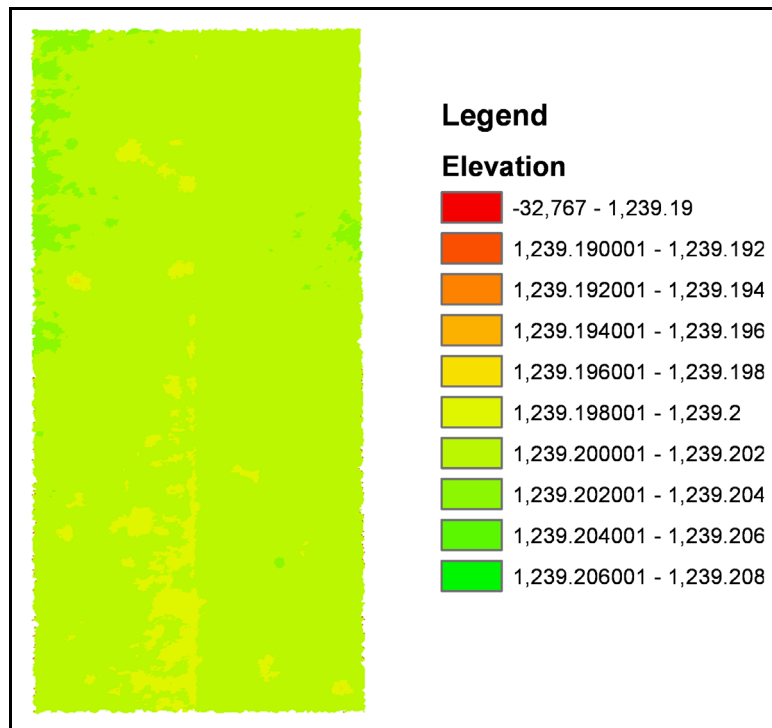
Figure A.6: DEM of Hairline Crack at 2 ft (61 cm) away using 15 Photos Displayed in ArcGIS
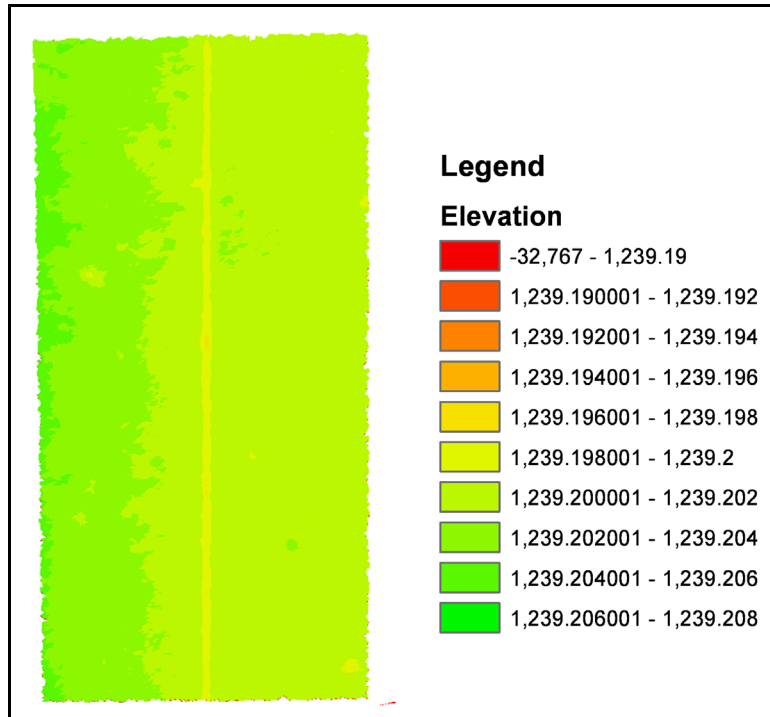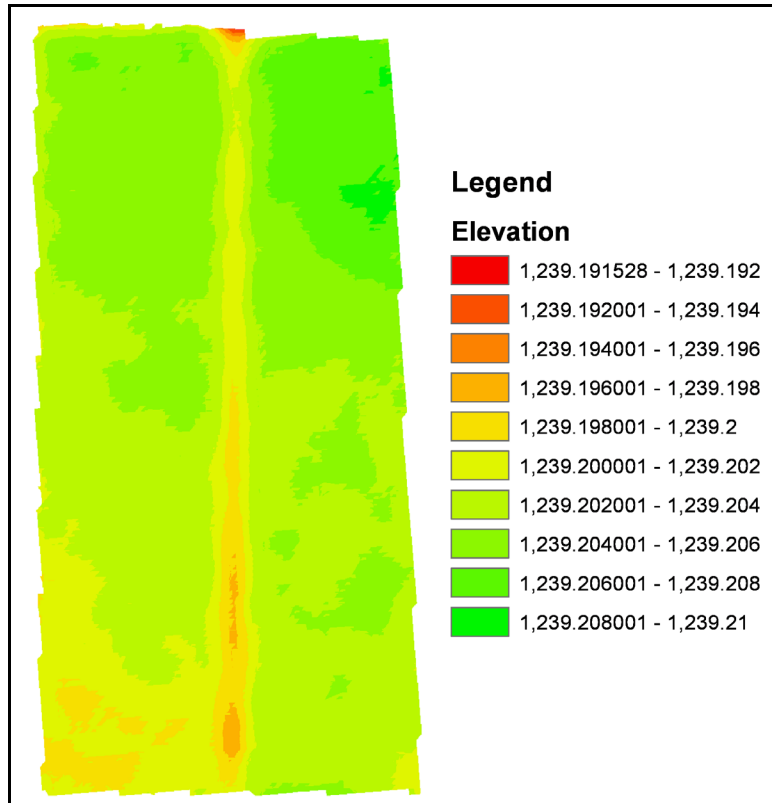
Figure A.7: DEM of 1/8 in. (3.18 mm) Crack at 2 ft (61 cm) away using 15 Photos Displayed in ArcGIS
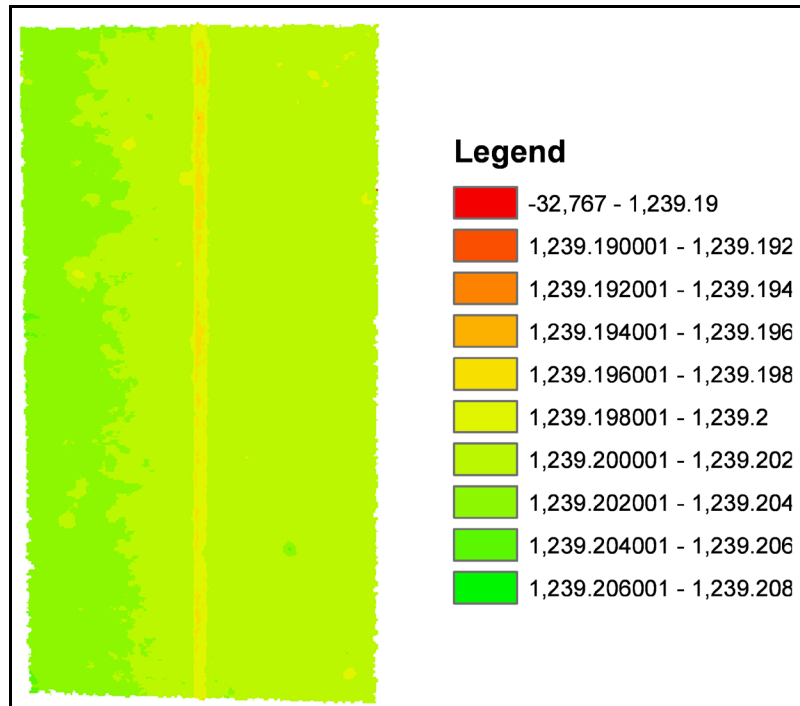
Figure A.8: DEM of 1/4 in. (6.35 mm) Crack at 2 ft (61 cm) away using 15 Photos Displayed in ArcGIS
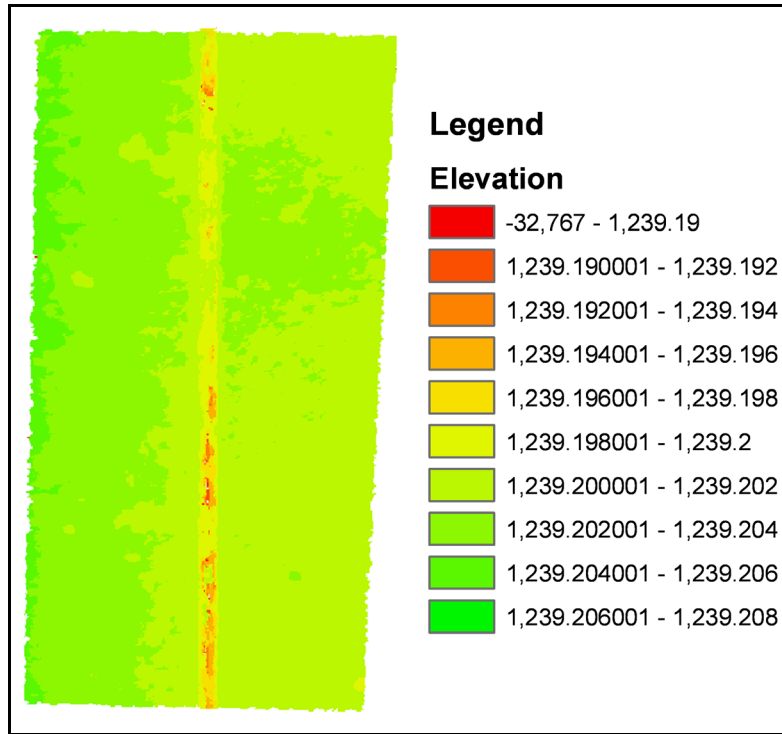
Figure A.9: DEM of 3/8 in. (9.53 mm) Crack at 2 ft (61 cm) away using 15 Photos Displayed in ArcGIS
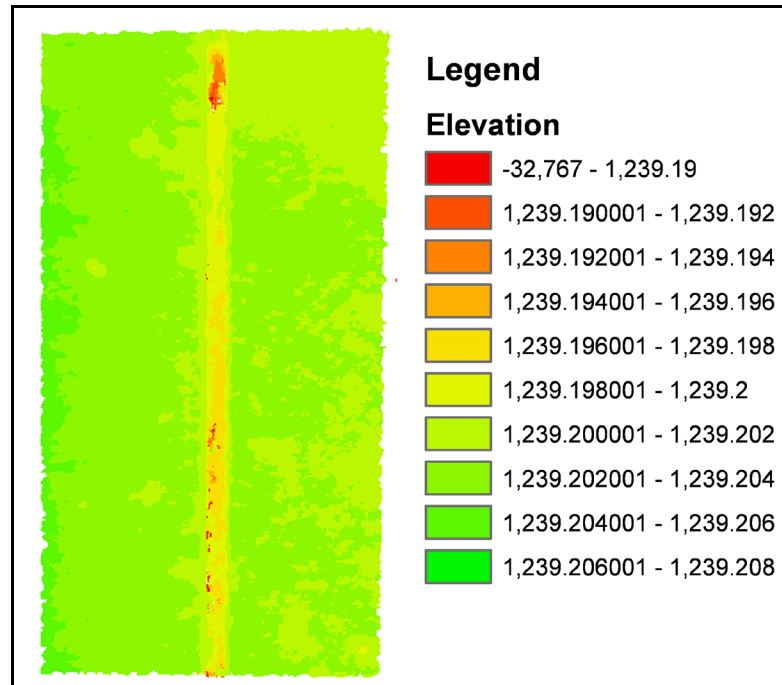
Figure A.10: DEM of 1/2 in. (12.7 mm) Crack at 2 ft (61 cm) away using 15 Photos Displayed in ArcGIS
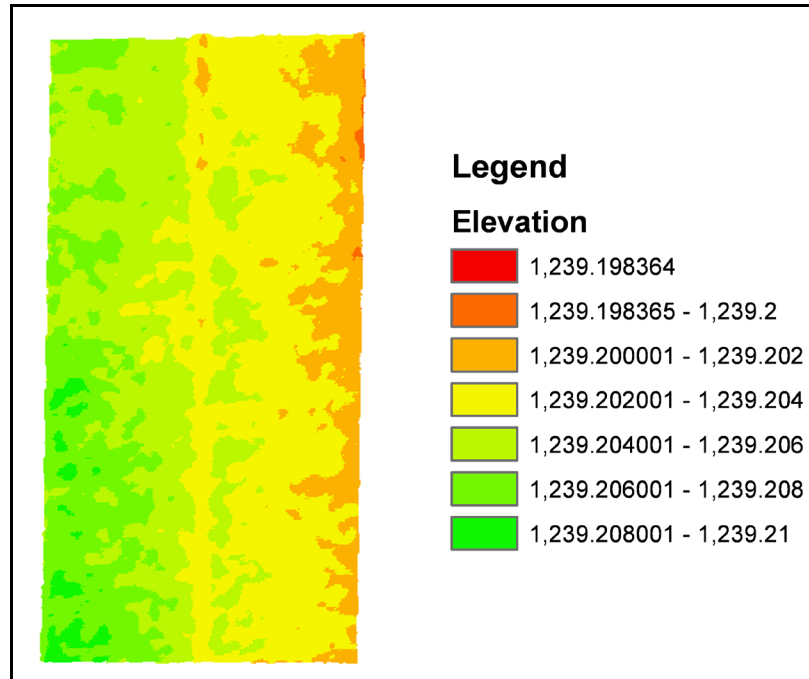
Figure A.11: DEM of Hairline Crack at 5.5 ft (1.68 m) away Displayed in ArcGIS
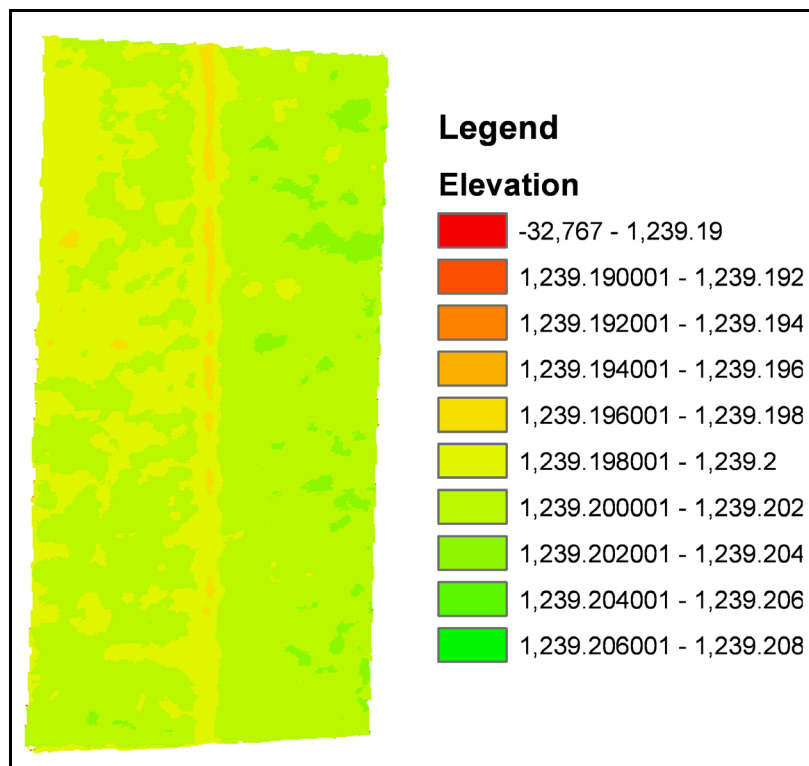
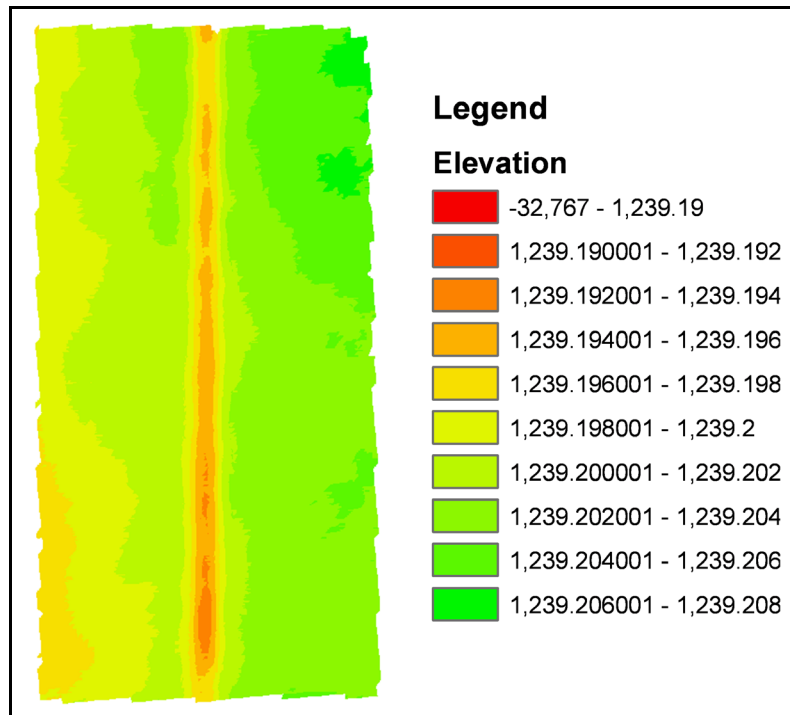**Figure A.12: DEM of 1/8 in. (3.18 mm) Crack at 5.5 ft (1.68 m) away Displayed in ArcGIS**
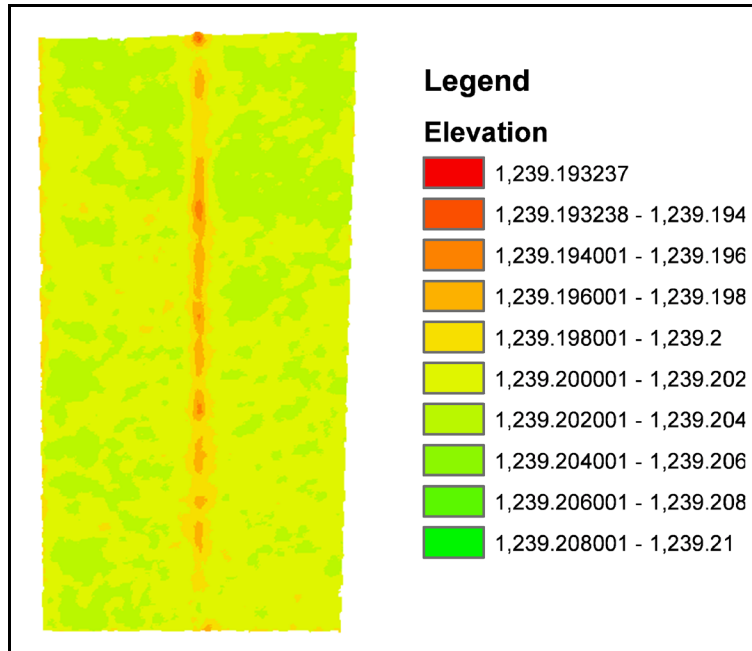
Figure A.13: DEM of 1/4 in. (6.35 mm) Crack at 5.5 ft (1.68 m) away Displayed in ArcGIS
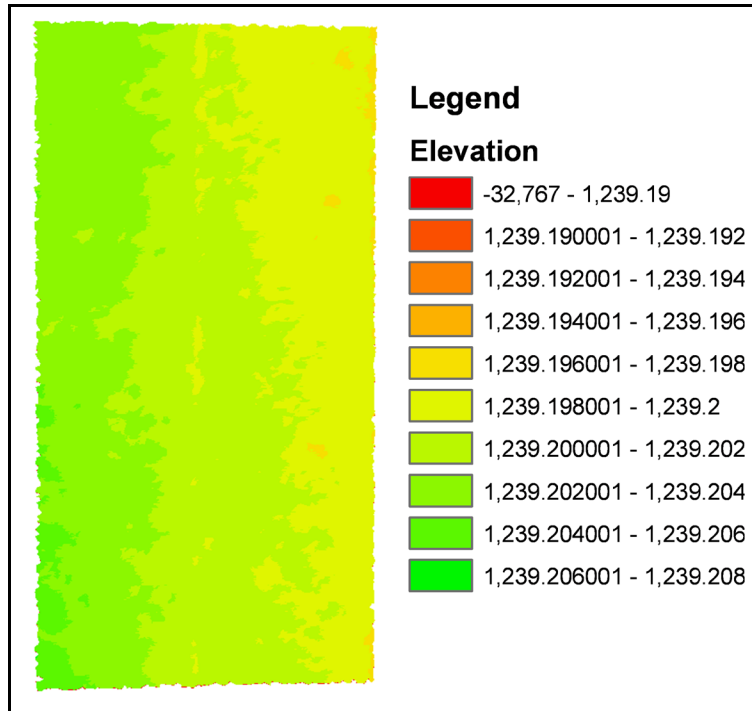

Figure A.14: DEM of 3/8 in. (9.53 mm) Crack at 5.5 ft (1.68 m) away Displayed in ArcGIS

Figure A.15: DEM of 1/2 in. (12.7 mm) Crack at 5.5 ft (1.68 m) away Displayed in ArcGIS
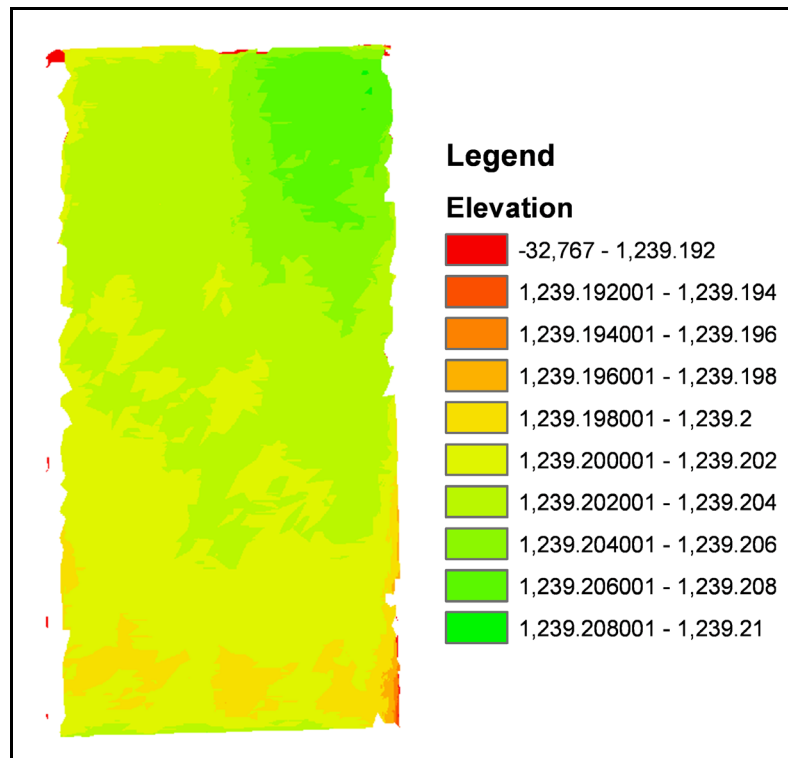
Figure A.16: DEM of Hairline Crack at 11 ft (3.35 m) away Displayed in ArcGIS
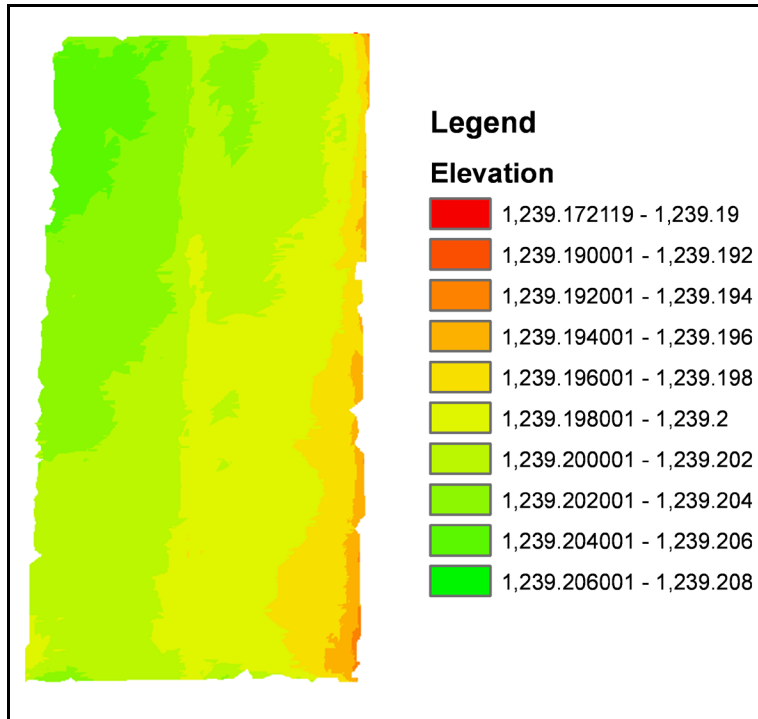
Figure A.17: DEM of 1/8 in. (3.18 mm) Crack at 11 ft (3.35 m) away Displayed in ArcGIS

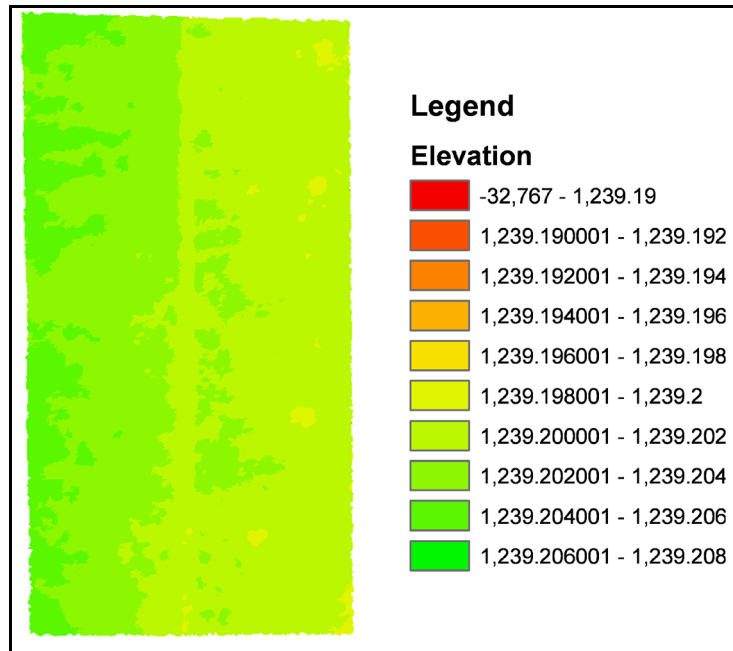**Figure A.18: DEM of 1/4 in. (6.35 mm) Crack at 11 ft (3.34 m) away Displayed in ArcGIS**

Figure A.19: DEM of 3/8 in. (9.53 mm) Crack at 11 ft away Displayed in ArcGIS
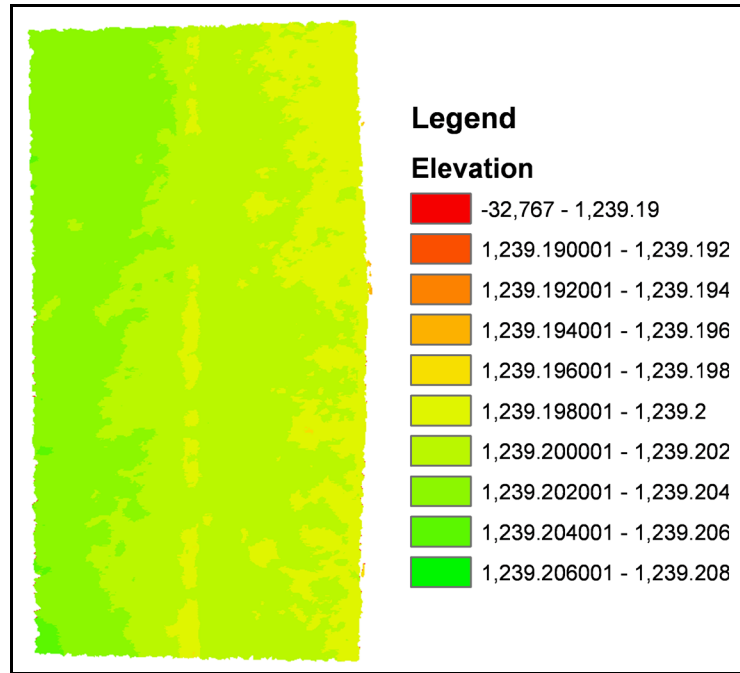

Figure A.20: DEM of 1/2 in. (12.7 mm) Crack at 11 ft away Displayed in ArcGIS
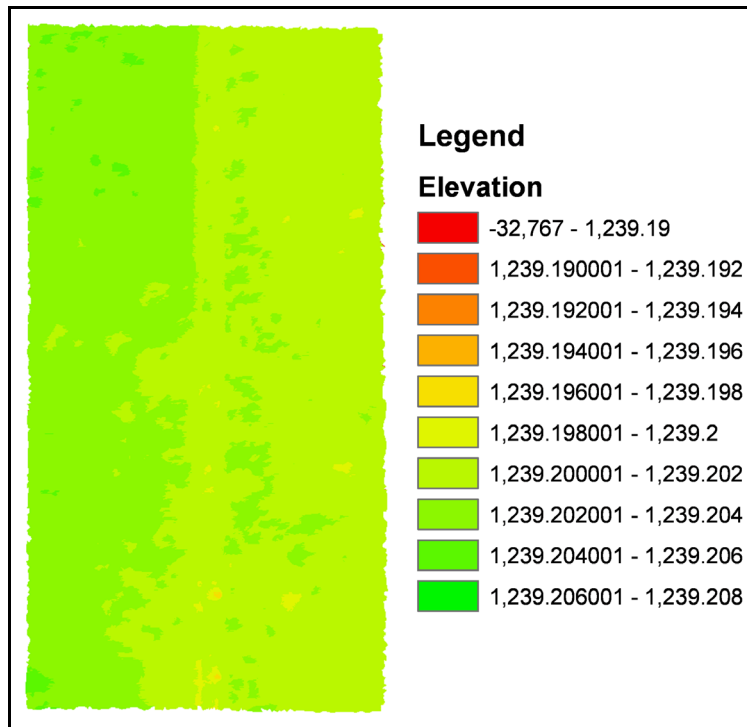
69

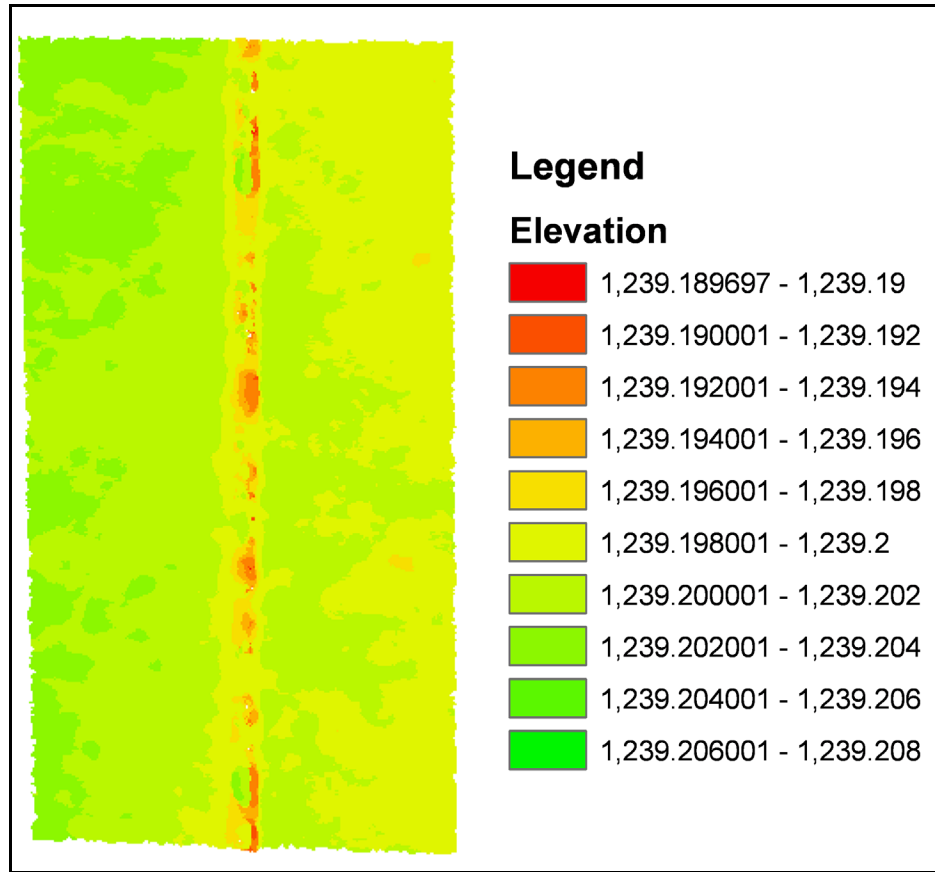**Figure A.21: DEM of Hairline Crack at 2 ft (61 cm) away with a 45 Degree Angle Displayed in ArcGIS**

Figure A.22: DEM of 1/8 in. (3.18 mm) Crack at 2 ft away with a 45 Degree Angle Displayed in ArcGIS

Figure A.23: DEM of 1/4 in. (6.35 mm) Crack at 2 ft (61 cm) away with a 45 Degree Angle Displayed in ArcGIS

Figure A.24: DEM of 3/8 in. (9.53 mm) Crack at 2 ft (61 cm) away with a 45 Degree Angle Displayed in ArcGIS

71

Figure A.25: DEM of 1/2 in. (12.7 mm) Crack at 2 ft (61 cm) away with a 45 Degree Angle Displayed in ArcGIS